MSc

2.º
CICLO

FCUP
2021

Manipulation of growth conditions ofcyanobacteria to potentiate the production of high-value compounds for obesity treatment

Mariana Miranda Moutinho

U.PORTO

FACULDADE DE CIÊNCIAS
UNIVERSIDADE DO PORTO

Manipulation of growth conditions of cyanobacteria to potentiate the production of high-value compounds for obesity treatment

Mariana Miranda Moutinho

Dissertação de Mestrado apresentada à
Faculdade de Ciências da Universidade do Porto em
Aplicações em Biotecnologia e Biologia Sintética

2021

U.PORTO

FACULDADE DE CIÊNCIAS
UNIVERSIDADE DO PORTO

MSc

Manipulation of growth conditions of cyanobacteria to potentiate the production of high-value compounds for obesity treatment

Mariana Miranda Moutinho

Mestrado em Aplicações em Biotecnologia e Biologia Sintética

Departamento de Química e Bioquímica e Departamento de Biologia

2021

Supervisor

Ralph Urbatzka, Researcher, Interdisciplinary Centre of Marine and Environmental Research (CIIMAR)

Co-supervisor

Vítor Vasconcelos, Full Professor, Faculty of Sciences of the University of Porto (FCUP)

Todas as correções determinadas
pelo júri, e só essas, foram efetuadas.

O Presidente do Júri,

Porto, _____/_____/_____

Acknowledgments

At the end of such an important stage in my academic and personal life, I would like to thank all the people that made it possible.

To my supervisor, Dr. Ralph Urbatzka, I thank the patience, guidance and teachings provided throughout this year, especially during the writing of this thesis. I sincerely appreciate the openness to hear my opinions and proposals for the development of this work, which undoubtedly sharpened my critical thinking skills. I am also grateful for the kind words of encouragement given when everything seemed too difficult to accomplish.

To my co-supervisor, Professor Vítor Vasconcelos, I thank the opportunity to perform my master's dissertation in the Blue Biotechnology and Ecotoxicology laboratory (BBE).

To Natália, Tiago, Diogo, Fábio and Catarina, I thank the availability that they have always shown to help and guide during this year. Likewise, I thank the little group of "Ralph's new students" that slowly formed, for the sharing of frustrations, laughter and a couple of beers that made this year so much easier. A special thanks to my lab partner, Sara, who helped me so much during this year, in the laboratory and personal life, and, who against all odds, became a close friend. Unlikely friendships really are the best.

To the close friends I made during my university years, especially Melo, Torres, Sérgio, Tatiana, Catarina, Aníbal and Ângela, thank you for the friendship, advice, discussions, good and bad times, overall amazing memories. It was all worth it. To Inês, roommate and friend of almost 15 years and still growing strong, thank you for always being there for me. Truly a companionship like no other, "*retas*" are forever. To the friends from Bragança, thank you for being part of this journey, regardless of the distance.

To my family, thank you for the love and support. I am especially grateful to my parents and brother, who always believed in me and encouraged me when everything seemed impossible. Thank you for trusting in me and in my decisions. Without you none of this would be possible.

To the project ATLANTIDA (ref. NORTE-01-0145-FEDER-000040) for financing this work, supported by the Norte Portugal Regional Operational Programme (NORTE 2020), under the PORTUGAL 2020 Partnership Agreement and through the European Regional Development Fund (ERDF).

Abstract

Obesity is one of the leading causes of premature death worldwide. Pharmacotherapy is the commonly recommended second line of treatment for obese individuals following lifestyle changes, however there are dangerous secondary effects associated. Marine organisms, in particular cyanobacteria, are a huge reservoir of chemically diverse compounds with bioactivities towards numerous human diseases.

Cyanobacteria are capable of spectacular metabolic plasticity, synthetizing secondary metabolites in order to survive and prosper in all kinds of environments. Manipulation of culture conditions allows the potentiation of biomass growth, or the induction of production of desirable molecules. Thus, modifications in the biochemical composition of the cells are an indicator of altered metabolism. Understanding the culture conditions that allow maximum production of target metabolites without biomass loss is of major importance in order to turn natural products with pharmaceutical application economically competitive.

In this work, *Cyanobium* sp. LEGE 07173, a cyanobacteria with previously described anti-obesity activity, was exposed to several conditions of light and temperature and tested for lipid-reducing activity using zebrafish larvae. The aim was to discover the culture conditions that potentiated the anti-obesity activity, and hence the production of responsible metabolites. The metabolite profiles of extracts of interest was characterized by mass spectrometry (LC-MS/MS), and a molecular network was produced with the focus to compare active and non-active samples to identify unique metabolites.

The results of the light and temperature experiments suggested that the responsible metabolites are synthetized under neither stress nor optimal growth conditions, but that certain conditions need to be evaluated experimentally. In particular, temperatures at 14°C and 18°C with middle light intensities (150 µmol $m^{-2}s^{-1}$) and in extractions with dichloromethane:methanol followed by fractionation with hexane (A fractions, nonpolar compounds) revealed significant anti-obesity activity present in the strain LEGE 07173 ($p < 0.05$). The molecular networking allowed the putative identification of 7 MS/MS mass peaks (5 with a match in databases, 2 unknown), which were simultaneously unique to both active samples, but did not have previously described anti-obesity activity. Further experiments are needed to validate these results.

Keywords: obesity; cyanobacteria; secondary metabolites; culture conditions; lipid-reducing activity; zebrafish.

Resumo

A obesidade é uma das principais causas de morte prematura em todo o mundo. Farmacoterapia é a segunda linha de tratamento recomendada para indivíduos obesos após mudanças no estilo de vida, no entanto, está associada a efeitos secundários graves. Organismos marinhos, particularmente cianobactérias, são um reservatório de compostos qumicamente diversos, bioativos para numerosas doenças humanas.

As cianobactérias são capazes de uma enorme plasticidade metabólica, produzindo metabolitos secundários que lhes permitem sobreviver e prosperar em todos os tipos de ambientes. A manipulação das condições de cultura permite a potenciação do crescimento da biomassa, ou a indução da produção de moléculas desejáveis. Assim, modificações na composição bioquímica das células são um indicador de metabolismo alterado. Conhecer as condições de cultura que permitem a produção máxima de metabolitos-alvo sem perda de biomassa é de grande importância para tornar os produtos naturais com aplicação farmacêutica economicamente competitivos.

Neste trabalho, *Cyanobium* sp. LEGE 07173, uma cianobactéria com atividade anti-obesidade anteriormente descrita, foi exposta a várias condições de luz e temperatura e testada para atividade redutora de lípidos usando larvas de peixe-zebra. O objetivo era descobrir as condições de cultura que potenciavam a atividade anti-obesidade e, consequentemente, a produção de metabolitos responsáveis. Os perfis metabólicos de extratos de interesse foram caracterizados por espectrometria de massa (LC-MS/MS), e uma rede molecular foi produzida com o intuito de comparar amostras ativas e não ativas para identificação de metabolitos únicos.

Os resultados das experiências de luz e temperatura sugeriram que os metabolitos responsáveis não são sintetizados em condições de stress ou de crescimento ideais, mas certas condições têm de ser avaliadas experimentalmente. As temperaturas a 14°C e 18°C com intensidades de luz média (150 μmol $m^{-2}s^{-1}$) e em extrações com diclorometano:metanol seguidas de fracionamento com hexano (frações A, compostos apolares) revelaram atividade anti-obesidade significativa presente na estirpe LEGE 07173 ($p < 0,05$). A rede molecular permitiu a identificação putativa de 7 picos de massa MS/MS (5 com correspondência nas bases de dados, 2 desconhecidos), que eram únicos para ambas as amostras ativas, mas não tinham atividade anti-obesidade previamente descrita. São necessárias mais experiências para validar estes resultados.

Palavras-chave: obesidade; cianobactérias; metabolitos secundários; condições de cultura; atividade redutora de lípidos; peixe-zebra.

Table of contents

Tables index

Figures index

Abbreviations list

ATP	Adenosine triphosphate
BBE	Blue Biotechnology and Ecotoxicology
BMI	Body Mass Index
BOGA	Bioterium for Aquatic Organisms
BSA	Bovine Serum Albumin
C/EBPα	CCAAT – enhancer-binding protein α
CIIMAR	Interdisciplinary Centre of Marine and Environmental Research
CO_2	Carbon dioxide
DCM	Dichloromethane
DMNP	Dictionary of Marine Natural Products
DMSO	Dimethyl sulfoxide
DNP	Dictionary of Natural Products
DPF	Days post-fertilization
EC_{50}	Half maximal effective concentration
EMA	European Medicines Agency
FDA	Food and Drug Administration
FIMT	Fragment Ion Mass Tolerance
GLP-1	Glucagon-like peptide 1
GluTR	Glutamyl-tRNA reductase
GNPS	Global Natural Products Social Molecular Networking
GSA-AT	Glutamate 1-semialdehyde aminotransferase
HDL-C	High Density Lipoprotein Cholesterol
IC_{50}	Half maximal inhibitory concentration
LC-MS/MS	Liquid Chromatography with Tandem Mass Spectrometry
LED	Light Emitting Diode
LEGE-CC	Blue Biotechnology and Ecotoxicology Culture Collection
MAPK	Mitogen-activated protein kinases
MeOH	Methanol
MFI	Mean Fluorescence Intensity
MIP-6	Mytilus Inhibitory Peptide 6
MS-222	Tricaine methane sulfonate
NADP	Nicotinamide Adenine Dinucleotide Phosphate
NF-κB	Nuclear factor-kappa B
OD	Optical Density

TAG	Triacylglycerol
PIMT	Precursor Ion Mass Tolerance
POMC	Pro-opiomelanocortin
PPAR-γ	Peroxisome proliferator-activated receptor gamma
ppm	Parts per million
PSII	Photosystem II
PTU	Phenylthiourea
REV	Resveratrol
RIPA	Radioimmunoprecipitation assay
RiPP	Ribosomally synthesized and post-translationally modified peptide
ROS	Reactive Oxygen Species
SREBP1	Sterol regulatory element-binding protein 1
TLR4	Toll-line receptor 4
UCP-1	Uncoupling protein 1
UFI	Unit of Fluorescence Intensity
WHO	World Health Organization

Appendixes index

Introduction

1.1. Overview on obesity

Obesity is regarded as one of the most concerning public health issues of today. According to the World Health Organization (WHO), by 2016, there were 1.9 billion overweight adults, of which 650 million were obese (39% and 13% of the world population respectively). Excessive weight also affects the younger population: by 2016, 340 million children and teenagers were overweight or obese [1]. Being above a healthy weight at a young age is a risk factor for the persistence or development of obesity, as well as related diseases, and is estimated that about 90% of obese adolescents become obese adults [2]. In Portugal, the National Food, Nutrition and Physical Activity Survey of 2015-2016 revealed that almost 60% of the general population is obese or pre-obese, with particular incidence in the elderly, women and the less educated [3].

A commonly used assessment to define obesity is the body mass index (BMI), calculated through the division of a person's body weight in kilograms by the squared height in meters (kg/m^2). Obesity is defined by a BMI of ≥ 30 kg/m^2, and overweight is defined by a BMI of 25 – 29,9 kg/m^2 [4]. Obesity is characterized as an abnormal or excessive accumulation of fat, which may be a consequence of genetic susceptibility, positive energy balance, high caloric diet and/or sedentary lifestyle [5]. This fat accumulation occurs in adipocytes, either by their increase in number (hyperplasia) or by their increase in size (hypertrophy). Adipocytes are crucial regulators of the whole-body metabolism through the secretion of hormones that control energy homeostasis in peripheral tissues and insulin sensitivity [6]. Obesity involves the interaction of various organs and tissues (brain, muscles, pancreas, liver, intestine and adipose tissue), different metabolic and hormonal pathways, and even brain regulation of appetite and food uptake, thus being a complex metabolic disease [6, 7].

Several comorbidities are associated with obesity, such as diabetes mellitus, hyperlipidemia, infertility, hypertension, sleep apnea, along with an increased risk of various types of cancer (ovarian, endometrial, breast, colon and prostate cancer), coronary disease and unexplained heart failure [8]. Besides its physical consequences, obesity also influences the mental health of the individuals. The stigma surrounding this disease turns people more susceptible to eating, mood and motivational disorders, as well as low self-esteem, impaired body image and difficulties when it comes to interpersonal communication and relationships [9]. The combination of these factors renders obesity an extremely debilitating disease both from a physical and psychological

point of view. Hence, is no surprise that obesity is one of the leading causes of disability and premature death worldwide [8].

The limitations and health impacts imposed by obesity carry an economical burden, since people suffering from this disease tend to have less school attendance, reduced earning potential, and higher healthcare costs [10]. Furthermore, the increasing number of overweight and obese people translates in a loss of work value and consequently in a higher societal expense because these individuals have a tendency to perform less productively due to their absence from work, physical limitations, low life expectancy, disability pensions and unemployment benefits [11]. The global economic impact of obesity was estimated to be US $2.0 trillion or 2.8% of the global gross domestic product back in 2014 [12]. However, if the current trend persists, most of the adult world population will be overweight or obese by 2030, therefore the healthcare costs and overall economic impact of obesity will increase significantly [13].

The major negative effect of obesity in the quality of life of the individuals and in society as a hole is undeniable. As such, urgent measures from governments, food industry and even society itself are needed for the prevention and treatment of this disease [12].

1.2. Approaches for obesity treatment

Since there is no single cause for obesity, solving this disease can be difficult. Physical exercise and healthy eating are traditionally seen as solutions to this problem, and indeed are very important factors for obesity prevention. However, lifestyle changes alone may not be enough in many cases. Even though obesity may start as a lifestyle-driven issue, evidence suggests that it can lead to impaired hypothalamic signalling, resulting in disturbed energy-balance regulation and consequently leading to a higher body-weight set point [14]. Thus, although healthier diet and physical exercise are important, they may be insufficient, and should be complemented with other strategies to significantly promote weight loss and the improvement of obesity related diseases [6].

Bariatric or obesity surgery is an effective treatment for morbidly obese individuals (BMI of ≥ 40 kg/m^2 or ≥ 35 kg/m^2 with at least one comorbidity), resulting in sustained weight loss, as well as improvement and even remission of many comorbidities such as type 2 diabetes, obstructive sleep apnea, dyslipidaemia and hypertension [15]. However, there are risks associated with these procedures, including long-term vitamin and mineral deficiencies or even death. Moreover, there is a high possibility that other surgeries will

be needed after bariatric surgery, due to gastroduodenal ulcers, internal hernias, bowel obstruction and gastrogastric fistulas [15, 16]. The fact that this treatment is only available for the morbidly obese, together with the high costs and risks associated, makes these procedures only reliable for a fraction of the general obese population [17].

Currently, most guidelines recommend pharmacotherapy as a second line of treatment following lifestyle changes for patients with BMI ≥ 30 kg/m^2 or BMI ≥ 27 kg/m^2 with existing comorbidities. Anti-obesity drugs aim to reduce body weight by ≥ 5%, which was shown to decrease high glucose and/or triglyceride profiles, leading to an improvement of several comorbidities [4]. Over the years, numerous pharmaceuticals have been developed for the long-term management of obesity. However, most of them have been removed from the market due to dangerous side effects, namely cardiovascular-related issues. As such, the development of anti-obesity drugs has been focusing not only on weight loss efficiency but also cardiovascular safety [18].

Regarding their mechanism of action, anti-obesity drugs can be divided into four groups: drugs suppressing appetite, drugs increasing insulin sensitivity, drugs targeting sodium/glucose co-transporters and drugs decreasing lipid absorption [19]. Today, five pharmaceuticals are approved by the FDA (Food and Drug Administration), three of which are also EMA (European Medicinal Agency) approved: orlistat, the naltrexone/bupropion combination and liraglutide [4, 18].

Orlistat is a hydrogenated derivative of lipstatin, a natural occurring lipase inhibitor, isolated from the bacterium *Streptomyces toxytricini*. This drug works by inhibiting the activity of the gastrointestinal and pancreatic lipases, decreasing fat absorption and therefore calorie intake [19]. This remains the only medication available for adolescents over 12 years of age [18]. Naltrexone is an μ-opioid receptor antagonist used in the treatment of alcohol and opioid addiction. It prevents the autoinhibition of hypothalamic POMC (pro-opiomelanocortin) neurons, which has anorexigenic effects. Bupropion is an anti-depressant and is also used in smoking cessation. This drug enhances the activity of POMC neurons. As a result, the combination of naltrexone with bupropion works synergistically, increasing satiety and supressing appetite [4]. Liraglutide is a glucagon-like peptide agonist with 97% homology to human GLP-1, firstly approved for the treatment of diabetes type 2 and later approved for obesity treatment. GLP-1 regulates blood glucose levels. Furthermore, it acts on the hypothalamus, limbic/reward system and cortex, inducing postprandial satiety and fullness and slowing gastric emptying, leading to appetite suppression. Liraglutide however, has a much longer half-life, further enhancing the normal GLP-1 activity. This allows the individuals to feel full for longer,

reducing their appetite and consequently their food consumption, which ultimately leads to weight loss [4, 18].

Although the risk to benefit ratio is considered acceptable, these drugs present adverse side effects and long-term complications such as gastroesophageal reflux disease, increased blood pressure, constipation, headache, dry mouth, heart disease, depression, nausea, liver failure, insomnia, psychiatric and cognitive effects, and even death [17]. Additionally, drug misuse, abuse and addiction have been reported [20].

Altogether, these factors demonstrate the urgency for the discovery and development of novel anti-obesity agents, leading to a more effective management of obesity [20]. Natural products have been an important source of agents with bioactivity against various disorders and diseases while producing less significant adverse effects [21]. Numerous natural products, including crude extracts, fractions and isolated compounds like secondary metabolites, from all types of organisms, such as aquatic and terrestrial plants, algae, bacteria, fungi and animals were described to have bioactivity properties valuable for the treatment and prevention of obesity [19, 22].

1.3. Marine natural compounds with anti-obesity activity

Nature represents a huge reservoir of biologically active compounds that is largely unexplored [17]. The marine world, in particular, provides a vast opportunity for exploring functional compounds due to high taxonomic and ecosystem diversity, and hence high chemo-diversity. The hostile environments to which marine organisms have to adapt, such as extreme temperature, high salinity and pressure, and hazardous pathogens, leads to the synthesis of metabolites that cannot be found in terrestrial organisms. Epidemic studies reveal a link between the consumption of seafood and a reduced prevalence of metabolic disorders such as obesity. Besides, many natural products from marine organisms were described for their potential as treatment of obesity [19, 23].

There are five major categories in which natural compounds with anti-obesity activity can be divided based on their mechanism of action: appetite or food intake suppression, lipase inhibition and consequent reduced lipid absorption, stimulation of energy expenditure (for example, through thermogenesis), regulation of lipid metabolism (either through decreased lipogenesis or increased lipolysis) and regulation of adipocyte differentiation and proliferation [17, 23].

Fucoxanthin is a carotenoid found in various species of brown macroalgae and cyanobacteria. It’s a well-established secondary metabolite with anti-obesity activity, with

known mechanisms of action, as well as recognized efficacy and safety in pre-clinical models as well as in clinical trials, reviewed by several articles [24-29]. This carotenoid decreases the expression of regulators involved in adipogenesis, such as PPAR-γ, C/EBPα, and SREBP1c, inhibiting intercellular lipid accumulation in a concentration of 10 µM in 3T3-L1 adipocytes [30]. Furthermore, it stimulates the expression of UCP-1 and β3-adrenergic receptor in white adipose tissue, leading to increased lipolysis and thermogenesis in KK-A^y mice fed a 0.1 and 0.2% fucoxanthin diet [31]. In a study conducted by Yim at.al, the anti-obesity activity of fucoxanthinol and amaraouciaxanthin A, metabolites from fucoxanthin, was tested in 3T3-L1 cells. Amarouciaxanthin A was found to suppress the expression of PPAR-γ and C/EBPα during adipocyte differentiation at 10 µM concentration to a greater extent that fucoxanthin, leading the authors to affirm that amarouciaxanthin A might be the molecule responsible for the anti-obesity effect of fucoxanthin [32].

Fucoidan is a sulphated polysaccharide present in brown algae and seaweed. Fucoidan isolated from *Undaria pinnatifida* suppresses adipogenesis through the inhibition of major adipocyte markers, inflammatory cytokines, and ROS production in 3T3-L1 cells at 10 and 100 $\mu g.mL^{-1}$ final concentration [33]. Recently, high-fat diet-induced obese mice daily treated with fucoidan dissolved in saline solution in a concentration of 10 mg/(kg.day) for 16 weeks showed inhibition of adipocyte hypertrophy and inflammation in adipose tissue [34].

Alginates are the major plant fibre isolated from the cell wall of brown seaweeds. This polysaccharide affects several physiological processes controlling food intake due to its ability to viscosify and form a gel within the gastrointestinal tract [35, 36]. Alginate was shown to supress glucose absorption by reducing gastric emptying and nutrient absorption through the viscosification of gastric contents in rats fed an alginate 5-10% diet, ultimately leading to weight loss [37].

Ethanol extract from the red seaweed *Gelidium amansii* was reported as having inhibitory effects in differentiation of 3T3-L1 adipocytes and protecting against high-fat diet-induced obesity in mice [38]. Another study revealed that supplementation with *Gelidium amansii* hot-water extracts produces beneficial effects on reducing body-weight and adipose tissue, plasma total cholesterol and triglyceride levels, triglyceride content in adipose tissue, and hepatic lipid accumulation on obese hamsters [39].

Caulerpa okamurae is a green macroalgae rich in minerals, fiber, vitamin A, vitamin C, alkaloids, β-sitosterol and essential unsaturated fatty acids [40]. A study conducted by Sharma et al. revealed that extracts from this seaweed decreased body and adipose

tissue weight, and plasma hepatic lipid profiles in high-fat diet-induced mice via regulation of adipogenesis, in addition to strongly inhibit lipid accumulation in 3T3-L1 adipocytes and reduce the expression of PPAR-γ and C/EBPα [41].

1.4. The role of cyanobacteria in the treatment of obesity

Cyanobacteria are an ancient group of gram-negative prokaryotes essential in the global carbon cycle as important primary producers performing oxygenic photosynthesis. These organisms present small cell size, can be unicellular, filamentous, or colonial, and display a wide geographical distribution, inhabiting all types of terrestrial and aquatic environments, ranging from deserts to freshwater and marine systems. They can also be found in extreme environments such as Antarctic dry valleys, Arctic and thermophilic lakes [42-44].

In order to adapt to this multitude of habitats, cyanobacteria developed interactions with several organisms, leading to the production of unique secondary metabolites [43]. Although some of this metabolites are toxic, many of them have promising therapeutic properties [45]. Thus, cyanobacteria have been considered a rich source of secondary metabolites with potential biotechnological applications in the pharmacological field. The possibility of production of bioactive compounds with commercial and medical applications has led to an increased interest in studying these organisms in the latter years [46]. In particular, several molecules were approved as clinical drugs for the treatment of cancer (https://www.marinepharmacology.org/approved).

Cyanobacteria contain several bioactive components that have potential benefits in obesity treatment and prevention, such as carotenoids, γ-linoleic acid, phycocyanin, fibres, and plant sterols [19]. Some strains of cyanobacteria are available over-the-counter, being *Arthrospira* sp., commonly known as *Spirulina*, one of the most significant. Many studies emphasise the anti-obesity properties of this cyanobacteria. *Spirulina* supplementation was shown to decrease white adipose tissue weight and normalize high density lipoprotein cholesterol (HDL-C) in C57BL/6J mice fed with a high-fat diet [47]. In another study, 13^2 – hydroxy – pheophytin a, a chlorophyll derivate, found in large quantities in *Spirulina* and other cyanobacteria, displayed significant lipid-reducing activities in zebrafish larvae and multicellular spheroids of differentiated 3T3-L1 adipocytes, in addition to altering PPAR-γ mRNA expression [48]. A study developed by Zhao et al. revealed that the *Arthrospira platensis* protein hydrolysate has superior anti-obesity effects than the whole *Spirulina*, reducing weight gain and total cholesterol, by modulating the expression of key genes in the brain and liver associated with lipid

metabolism in C57BL/6J mice [49]. Furthermore, clinical trials suggest that *Spirulina* supplementation significantly reduces body weight, body fat percentage and waist circumference, especially in obese individuals [50].

Many other species of cyanobacteria have been a subject of study in the discovery of compounds with anti-obesity activity. Recently, a screening of 263 fractions from different cyanobacterial species revealed that some of this fractions had potent effects on intestinal lipid absorption in zebrafish larvae *in vivo* with no toxic effects [51]. Yoshinone A, a compound isolated from *Leptolyngbya* sp., has shown supressing activity of the adipogenic differentiation in 3T3-L1 mice cells. The mechanism of action of this cyanobacterial compound is not well understood, nevertheless, the position of the γ-pyrone ring in the side chain is important to exhibit this bioactivity [52]. Another γ-pyrone, kalkipyrone, was effective in supressing adipose tissue weight in mice via oral ingestion [52]. Finally, diet supplementation with *Nostoc commune var sphaeroides Kützing* (*N. commune*) demonstrated cholesterol reducing activity, decreased intestinal cholesterol absorption and stimulated fecal sterol excretion in mice [19].

1.5. Culture conditions and cyanobacterial biochemical composition

Besides bioactive compounds with pharmaceutical application, cyanobacteria are also a source of many interesting macromolecules with other biotechnological applications [53]. For instance, microalgae, including cyanobacteria and eukaryotic algae, can be used as environmental agents, either by their ability to capture and fixate carbon dioxide during photosynthesis, or by uptake of nitrogen and phosphate in wastewater treatment [54]. Furthermore, environmental concerns regarding the usage of fossil fuels has urged the search of renewable and environmentally friendly fuels. Microalgae are considered some of the most promising feed stocks for such fuels, due to their high growth rate and decreased land requirements when compared to other resources. Many of these organisms produce significant amount of lipids that can be converted to biodiesel, and carbohydrates that can be converted to bioethanol [54-56]. Nonetheless, the high-costs associated with microalgae-based fuels has significantly restricted their industrialization and economic attractiveness, leading to the proposal of biofuels production associated with high-value products (like metabolites for medical application) for microalgal biorefinery [57].

Regardless of the motive to grow microalgae, it is imperative to obtain sufficient biomass to extract satisfactory amounts of the compound of interest. Therefore,

cultivation is one of the most important processes in the usage of microalgae, particularly in order for these biotechnologies to become economically competitive [54, 56].

Cyanobacteria are primarily composed of proteins, carbohydrates, lipids and nucleic acids in different proportions. They also contain polysaccharides, minerals, vitamins and pigments such as chlorophylls and carotenoids. This composition is species/strain specific, but also varies with the growth conditions to which cyanobacteria are exposed [58]. Cyanobacteria growth is dependent on several factors, such as pH, nutrients availability, CO_2 supply, temperature and light conditions, as well as photoperiod [56]. Given the metabolic plasticity of these organisms, they can easily adapt to non-optimal conditions by changing their metabolic pathways and, as a result, increase or decrease the production of certain metabolites [53, 59]. In fact, it is speculated that secondary metabolites are originated as consequence of mechanisms of action against biotic or abiotic stress, as they serve no obvious function in the cell in addition to the fact that their synthesis requires extra energy, carbon and nitrogen allocation [58, 59].

Hence, exposing cyanobacterial cultures to different conditions will result in variations in the biochemical composition of the cells and, potentially, influence the synthesis of bioactive metabolites [54, 57, 59]. However, cyanobacteria exposure to stress conditions has limitations, given the frequent negative impact on cyanobacteria growth. Photosynthesis causes damage to photosynthetic organisms, particularly to photosystem II (PS II). Although organisms are equipped with reparation mechanisms, these photoprotection responses are affected by environmental stress, often leading to photoinhibition, and consequent growth declines or even cell death [60-62]. Hence, subjecting cyanobacteria to stressful environments may decrease biomass production and eventually lower the yield of desired products, which reflects the importance of manipulating culture conditions to achieve improved accumulation of target metabolites and biomass [57, 59]. Optimization of production of target compounds under stress conditions is therefore of particular significance and more research is needed [53, 54].

1.6. Zebrafish as a model organism for obesity research

For the discovery of new compounds with anti-obesity activity, it is essential to use a suitable model organism. The screening for novel compounds is traditionally performed *in vitro* [6]. Cell lines, like the 3T3-L1 preadipocyte, are cost-effective, reproducible, and can be passaged a number of times, allowing a continuous supply of preadipocytes [63]. However, the interplay between different tissues and organs, which is of crucial

importance in the evolution of metabolic diseases, cannot be reproduced *in vitro*. Consequently, most of the hits generated by traditional screening turn out to be invalid, due to absorption, solubility, distribution, metabolic stability and toxicological problems in later animal studies [64].

Being a complex disease, obesity involves the interaction of different organs and tissues, such as adipose tissue, intestine, brain and liver. Consequently, using a complex organism will be beneficial to produce more physiologically relevant results than an *in vitro* cell culture in the study of obesity and drug research [6]. Still, the utilization of mammalian models, like rodents, comprises disadvantages such as ethical issues, high cost and maintenance [65]. Common non-mammal models in obesity research are *Caenorhabditis elegans*, *Drosophila melanogaster* and *Danio rerio*. The use of these organisms presents several advantages, such as short life and reproductive cycle, high fecundity, low-maintenance cost and easy handling [66-68].

C.elegans is a free-living nematode with more than 65% of the genes associated with human disease. Besides, there are over 3000 mutant strains available for biomedical research. However, this organism holds significant disadvantages such as lack of particular organs and circulatory system and lower conservation of biological pathways with humans compared to vertebrate models [66]. Conversely, *Drosophila* contains tissues, organs and systems analogous to those involved in human obesity, developing obesity themselves, and related complications, during caloric overload. Moreover, most genes and gene families associated with metabolic disease are conserved between flies and humans [67]. Nevertheless, as ectotherms, flies do not have to maintain body temperature, expending more energy on growth and reproduction than endotherms. As a consequence, physiological differences may be observed regarding the relationship between diet, energy expenditure and animal growth. Moreover, *Drosophila* models of drug discovery may be limited due to differences in drug metabolism pathways between flies and humans [69].

Zebrafish (*Danio rerio*), a freshwater teleost, has several similarities to mammals, including white adipose tissue and adipocytes cellular anatomy, all key organ systems regulating metabolism and energy homeostasis, as well as insulin and appetite regulation [68]. As in mammals, obese zebrafish undergo alterations in pathways related to lipid metabolism [5, 70]. Despite being a vertebrate, and therefore retaining characteristics similar to those of humans, this organism offers many of the advantages of invertebrate organisms, such as *C. elegans* and *Drosophila* [68]. In addition, embryonic development is external and both embryos and larvae are transparent, which

allows the monitoring of the evolution of organs over time and the application of fluorescence techniques and real-time imaging [5]. There's also hundreds of mutant and transgenic lines available for biotechnological and pharmaceutical research [71].

Due to their characteristics, zebrafish larvae emerge as an attractive model for high-throughput screening of bioactive compounds and the consequent discovery of new therapies for various diseases, namely, metabolic diseases [71]. A common procedure used in the discovery of anti-obesity compounds is the Nile Red fat metabolism assay, which analyses the neutral lipid-reducing activity in the yolk-sac of zebrafish larvae [72]. When it was first applied, it was concluded that this model presents signal transduction pathways that regulate lipid metabolism conserved among zebrafish and mammals and can thus be used to identify molecules for the treatment of obesity [72]. Despite its undeniable advantages, zebrafish has its limitations, including the fact that it is an ectothermic organism with genome duplication, which can affect its metabolic and neuroendocrine regulation, and the absence of brown fat tissue [73].

The capacity for in-depth phenotyping when it comes to physiology and tissue-specific biochemistry of metabolic diseases still falls short regarding the level of resolution in rodents [74]. Yet, zebrafish provide a powerful complementary platform, allowing the identification of compounds that can be latter validated on mammals, representing an intermediate step in obesity research between *in vitro* and rodent assays [74, 75].

1.7. Objectives

The main objective of this work was to manipulate the growth conditions of *Cyanobium* sp. LEGE 07173, a cyanobacteria with previously reported 50% lipid reduction at 10 $\mu g.mL^{-1}$ final concentration in zebrafish bioassays [76], in order to identify and optimize the production of responsible secondary metabolites. The specific objectives were to analyse the effects of the culture conditions on various biochemical parameters, and on the bioactivity of the extracts and fractions on obesity. Furthermore, metabolite profiling should give insights into the identification of compounds responsible for the anti-obesity activity.

To that effect, the cyanobacteria LEGE 07173 was grown under a variety of light and temperature conditions in photobioreactors, and several biochemical parameters were examined. Then, the cultures were extracted and fractionated, and the fractions tested for lipid-reducing activity in the zebrafish Nile Red fat metabolism assay. The

metabolite profile of extracts of interest was characterized by mass spectrometry (LC-MS/MS), and a molecular network was generated comparing active and non-active samples. In total, this work should contribute to the discovery of the secondary metabolites responsible for the observed anti-obesity bioactivity in the cyanobacterial strain LEGE 07173.

2. Materials and Methods

2.1. Culture maintenance and growth

2.1.1. BOGA culture

The BBE (Blue Biotechnology and Ecotoxicology) team holds its own culture collection (LEGE-CC) with more than 1000 different strains of cyanobacteria and microalgae from marine, estuarine, and freshwater environments. The associated database contains information about these strains, including origin, taxonomic-related data, morphological description and culture conditions [77].

Based on results obtained in previous screening assays for bioactive compounds conducted by the BBE team, the strain *Cyanobium* sp. LEGE 07173, belonging to the Synechococcales order, was determined as promising for the production of compounds with lipid-reducing activity [76]. The cyanobacterium was cultured with Z8 culture medium, which integrates both macro and micronutrients (Appendix I), supplemented with 25 $g.L^{-1}$ of Tropical Marine salt and vitamin B12 [78], at 20 °C, under a light intensity of 80 – 125 $\mu mol\ m^{-2}s^{-1}$ and kept in the Bioterium for Aquatic Organisms (BOGA). The standard procedure was to initiate the culture in a new 50 mL culture flask. Then, a small amount of the culture was transferred to a 500 mL culture flask and the adjusted amount of Z8 medium was added. Finally, about 400 mL of the culture was transferred to an autoclaved 2L Erlenmeyer with the adjusted amount of Z8 medium, supplemented with air flux, for a continued medium circulation. The 50 mL and 500 mL culture flasks were kept in case of contamination of the bigger scale-up or for possible needed future scale-ups. For all the scale-ups, autoclaved deionized water with Tropical Marine salt and the adjusted amount of Z8 medium compounds were used and performed in sterile conditions using a Telstar Bio II Advance laminar flow chamber.

The cyanobacterial biomass was harvested through centrifugation in a Thermo Scientific Sorvall Bios 16 at 5000 g at 4°C for 20 minutes. Because this is a marine strain, an additional washing step with deionized water was added in order to remove the salt from the biomass. The pellet was kept at -20°C and latter freeze-dried in a Telstar LyoQuest.

2.1.2. Algem® cultures

In order to understand how different light and temperature conditions affect the metabolic profile and bioactivity of the cyanobacteria, the Algem® labscale photobioreactor (Algenuity) was used. Each of the three systems (system 1, 2 and 3) available at CIIMAR contain two individually programable photobioreactors

(photobioreactor A and B) (Fig. 1), that allow the setting of specific conditions and the follow up of cultures over time. The controllable and programable parameters include precision lighting control, automated optical density (OD) measurement, computer control of pH via CO_2, and profiled control of light and temperature (including white, red and blue LEDs, and active heating and cooling). This is possible due to the Algenuity's own custom-designed Algenious user interface (Fig. 2) that displays acquisition of all major parameters simultaneously in real time.

Fig. 1 – Photobioreactors system Algem® by Algenuity.

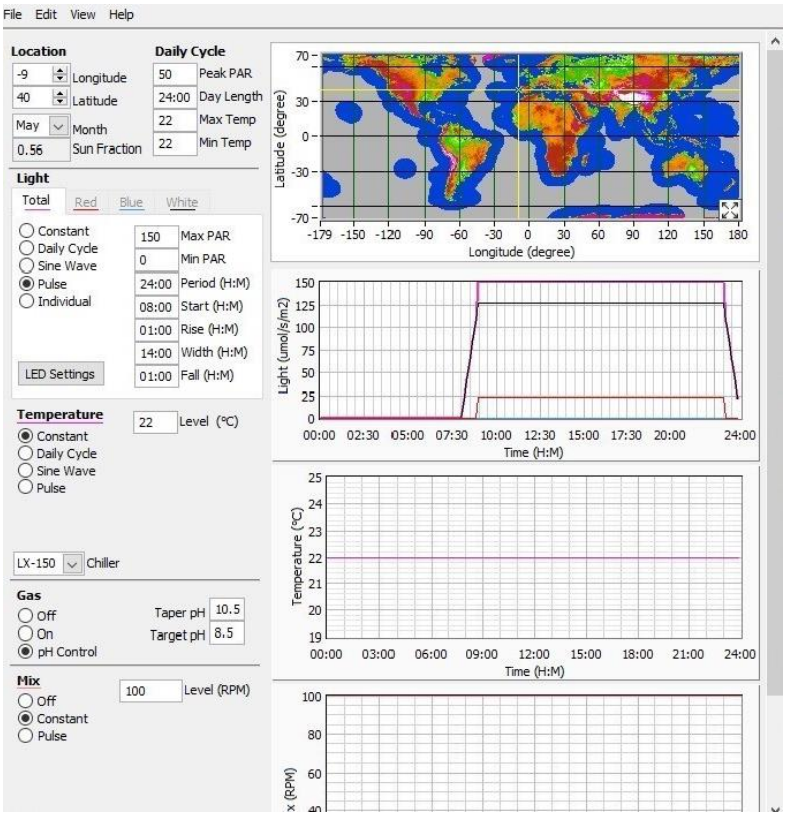

Fig. 2 – Algenious software layout.

The required amount of the BOGA culture, needed to achieve an initial OD of 1 (Biotek, Synergy HT plate reader) at 750 nm, was transferred to autoclaved Algem® 600 mL Erlenmeyer's with 600 mL of deionized water with Tropical Marine salt and the adjusted amount of Z8 medium compounds under sterile conditions using a Telstar Bio II Advance laminar flow chamber. The cultures were kept in the photobioreactors for 21 days, which allowed them to achieve stationary growth phase, at a constant pH of 8.5 and a photoperiod of 16 hours day:8 hours night (except for photobioreactor 2B in the light experiment, with a photoperiod of 24 hours day).

The culture conditions in the light experiment were as follows:

- Photobioreactor 1A – Sunlight (15% red, 85% white), 50 µmol $m^{-2}s^{-1}$, 25°C – Low light
- Photobioreactor 1B – Sunlight (15% red, 85% white), 150 µmol $m^{-2}s^{-1}$, 25°C – Middle light
- Photobioreactor 2A – Sunlight (15% red, 85% white), 500 µmol $m^{-2}s^{-1}$, 25°C – Strong light
- Photobioreactor 2B – Sunlight (15% red, 85% white), 150 µmol $m^{-2}s^{-1}$ 24 hours day, 25°C – Continuous light
- Photobioreactor 3A – Blue LED (85% blue, 15% white), 150 µmol $m^{-2}s^{-1}$, 25°C – Blue light
- Photobioreactor 3B – Red LED (85% red, 15% white), 150 µmol $m^{-2}s^{-1}$, 25°C – Red light

When this experiment was being initialized, an error was found in the pH probe of the photobioreactor 1A. As such, the experiment in this photobioreactor could not be started and this condition was not included.

The culture conditions in the temperature experiment were as follows:

- Photobioreactor 1A – 10°C, sunlight (15% red, 85% white), 150 µmol $m^{-2}s^{-1}$
- Photobioreactor 1B – 14°C, sunlight (15% red, 85% white), 150 µmol $m^{-2}s^{-1}$
- Photobioreactor 2A – 18°C, sunlight (15% red, 85% white), 150 µmol $m^{-2}s^{-1}$
- Photobioreactor 2B – 22°C, sunlight (15% red, 85% white), 150 µmol $m^{-2}s^{-1}$
- Photobioreactor 3A – 26°C, sunlight (15% red, 85% white), 150 µmol $m^{-2}s^{-1}$
- Photobioreactor 3B – 30°C, sunlight (15% red, 85% white), 150 µmol $m^{-2}s^{-1}$

2.2. Biochemical characterization

With the intention of obtaining preliminary results regarding how different light and temperature conditions affect the biochemical profile of the cyanobacteria, and, therefore, the type of metabolites synthetized, several biochemical parameters were tested.

2.2.1. Dry-biomass

A volume of 5 mL of each culture was diluted (1:5) in distilled water and filtered in pre-weighted 0.47 mm pore round cellulose filters with a vacuum pump (VRW, PM20405-86). Triplicates were made of each condition. The filters were left to dry for 24 hours at 60°C and weighted again (adapted from [76]). Dry-biomass was expressed in $g.L^{-1}$ of culture and used as a normalizing factor for the other biochemical parameters.

2.2.2. Protein content

A volume of 10 mL of each culture was placed in 15 mL falcon tubes. Triplicates were prepared. The falcon tubes were centrifuged at 5000 g at 4°C for 8 minutes in a Thermo Scientific Megafuge 16R. The supernatant was discarded. 200 µL of RIPA buffer in a 1:10 dilution was added to the pellets, dissolved by vortex and pipetting, and transferred to 2 mL Eppendorf tubes. The pellets were further dissolved by a hand-hold ultrasonicator (Vibra Cell VC50 Sonics & Materials Inc. Danbury, CT. USA), 10 times 1x pulse with 1 second interval, and left on ice for 30 minutes. Then, the samples were centrifuged at 17000 g at 4°C in a centrifuge (VWR, Micro Star 17R). The supernatants were transferred to new Eppendorf's and the pellets were discarded. To measure protein quantity, the supernatants were diluted with distilled water (1:10 dilution). In a 96 well plate, 195 µL of Bradford reagent were added to the needed wells, followed by 5 µL of the diluted supernatants. Bovine Serum Albumin (BSA) standards were used for a standard curve in duplicates (7 BSA standards prepared in RIPA buffer, serial 2-fold dilutions, 20 mg/mL – 0.3 mg/mL), and two blanks were prepared using RIPA buffer. The absorbance was measured at 595 nm using a plate reader (Biotek, Synergy HT) (adapted from [79]).

The BSA standard curve follows a logarithmic function of the type $y = m.\ln(x) + b$ in which y corresponds to the measured absorbance, x corresponds to the protein concentration, and m and b correspond to the slope and origin of the curve, respectively. Thus, once the equation of the curve was obtained, it was possible to calculate the protein concentration in $mg.mL^{-1}$ of each sample using the absorbance measured through spectrophotometry. The protein concentration was then normalized to the unit g of protein/g of dry-biomass.

2.2.3. Carbohydrate content

A volume of 5 mL of each culture was placed in 15 mL falcon tubes. Triplicates were prepared. The falcon tubes were centrifuged at 5000 g and 4°C for 8 minutes in a Thermo Scientific Megafuge 16R and the supernatant was discarded. The pellet was mixed by vortex and pipetting with 200 µL of distilled water. In a 96 well plate, 50 µL of each sample, 150 µL of 98% w/w H_2SO_4 and 30 µL of 5% w/v phenol were added in this order. Glucose standards were used for a standard curve in duplicates (8 standards prepared in distilled water, serial 2-fold dilutions, 8 mM – 0.0625 mM), and two blanks were prepared using distilled water. The plate was incubated for 10 mins at 60°C and then the absorbance was measured at 490 nm using a plate reader (Biotek, Synergy HT) (adapted from [80]).

The glucose standard curve follows a first-degree polynomial function or linear function of the type $y = m.x + b$ in which y corresponds to the measured absorbance, x corresponds to the carbohydrate concentration, and m and b correspond to the slope and origin of the curve, respectively. Thus, once the equation of the curve was obtained, it was possible to calculate the carbohydrate concentration in mM of each sample using the absorbance measured through spectrophotometry. The carbohydrate concentration was then normalized to the unit g of carbohydrate/g of dry-biomass.

2.2.4. Lipid content

A volume of 200 µL of each culture was added to wells in a 96 well plate in triplicates. 2 µL of Nile red, in a final concentration of 5 $\mu g.mL^{-1}$, were added. Blanks were prepared in triplicate using Z8 medium. The plate was incubated for 10 minutes in room temperature, and finally, Nile red fluorescence was read (excitation wavelength at 488 nm and emission wavelength at 640 nm) using the BioTek Cytation 5 (adapted from [81]). The lipid content was then normalized to the UFI (unit of fluorescence intensity)/g dry-biomass.

2.2.5. Pigments

A volume of 200 µL of each culture was added to wells in a 96 well plate in triplicates. Absorbance was directly read in the BioTek Cytation 5: chlorophyll a (652.4 nm), chlorophyll b (665.2 nm), and carotenoids (470 nm) (adapted from [82]). Each pigment content was then normalized to the unit Abs/g dry-biomass.

The remaining culture volume after the biochemical characterization was used for biomass harvesting as described above in 2.1.1. Furthermore, the data were statistically analysed for significant differences among the different conditions.

2.3. Extraction and fractionation

The light experiment cultures were extracted using methanol as organic solvent. All of the freeze-dried biomasses from the culturing in photobioreactors – 1B (36.9 mg); 2A (42.6 mg); 2B (62.1 mg); 3A (80.5 mg); 3B (38.3 mg) – were sonicated in 50 mL of MeOH using an ultrasonic bath for 10 minutes to lyse the cells. This process was repeated two more times using 25 mL of MeOH. The solvent was evaporated from the crude extracts using a rotavapor under vacuum at 30°C followed by a vacuum system overnight. The mass of crude extracts obtained – 1B (14.4 mg); 2A (12.4 mg); 2B (10.2 mg); 3A (14.1 mg); 3B (10.4 mg) – corresponds to an extraction yield of about 45%, 35%, 50%, 55% and 50% respectively.

The BOGA culture was submitted to two different types of organic extraction: one using methanol and the other using dichloromethane:methanol. In this methanolic extraction (M), the freeze-dried biomass of *Cyanobium* sp. LEGE 07173 (1162.8 mg) was firstly sonicated in 25 mL of MeOH using an ultrasonic bath for 15 minutes to lyse the cells. The biomass was then exhaustively extracted using MeOH (10 x 25 mL) until the mixture became transparent. The solvent was evaporated from the crude extract using a rotavapor under vacuum at 30°C followed by a vacuum system overnight. Through this process, 226.46 mg of crude extract were obtained, which corresponds to an extraction yield of about 20%.

In the dichloromethane:methanol extraction (DM), the freeze-dried biomass (790.7 mg) was firstly sonicated in 25 mL of MeOH using an ultrasonic bath for 15 minutes to lyse the cells. This process was repeated three times using MeOH, followed by four times using DCM in the same volume, until the mixture became transparent. The solvents were evaporated from the crude extract using a rotavapor under vacuum at 30°C followed by a vacuum system overnight. Through this extraction, 134.44 mg of crude extract were obtained, which corresponds to an extraction yield of about 18%.

The temperature experiment cultures were extracted similarly to the BOGA cultures extracted with DCM:MeOH. All of the freeze-dried biomasses – 1A (338.9 mg); 1B (448.5 mg); 2A (687.1 mg); 2B (773.7 mg); 3A (786.1 mg); 3B (700.4 mg) – were sonicated 3 times in 10 mL of MeOH using an ultrasonic bath for 15 minutes. The biomass was then extracted using 10 mL of DCM several times (7 times for 1A; 4 times for 1B; 6 times for 2B; 5 times for 2A, 3A and 3B) until the mixture became transparent. The solvents were evaporated from the crude extract using a rotavapor under vacuum at 30°C followed by a vacuum system overnight. The mass of crude extracts obtained – 1A (81.01 mg); 1B (112.95 mg); 2A (104.96 mg); 2B (145.79 mg); 3A (82.37 mg); 3B

(186.56 mg) – corresponds to an extraction yield of about 24%, 25%, 15%, 19%, 10% and 27% respectively.

All crude extracts were fractionated using a simple extraction protocol named increased polarity extraction (ABC). First, a silica column of 2 g or 5 g, depending on the mass of the crude extract (at least 30 – 40 times the mass of the extract), is activated using hexane, and then the extract diluted in 1 mL hexane is added to the column. The fractions were then obtained through sequential extraction with solvents of increasing polarity, hexane – nonpolar – (fraction A), ethyl acetate (fraction B) and methanol – polar – (fraction C). The solvents were evaporated from the fractions using a rotavapor under vacuum at 30°C followed by a vacuum system overnight. After they were dry, the fractions were diluted in DMSO in a final concentration of 10 $mg.mL^{-1}$ and stored at -20°C.

2.4. Zebrafish Nile Red fat metabolism assay

The zebrafish embryos were obtained from BOGA, where all aquatic organisms used in CIIMAR laboratories are maintained. The original procedure published by Jones *et al*. [69], optimized by the BBE team, was applied aiming the possible discovery of compounds with anti-obesity activity of the several fractions produced over the course of this work.

At the day of the fertilization – 0 DPF (days post fertilization) – the eggs were collected and cleaned manually, separating viable eggs from dead ones and impurities. The eggs were kept in an aquarium with dechlorinated water at 28°C. The day after, which corresponds to 1 DPF, the eggs were again cleaned and separated in petri dishes with 20 mL of egg water with PTU (phenylthiourea), at a maximum density of 40 eggs per petri dish and kept at 28°C. Egg water had a final concentration of 60 $\mu g.mL^{-1}$ salt and 200 µM PTU to suppress melanisation. On 3 DPF, 5 to 7 zebrafish larvae were added to the wells in a 48 well-plate. The fractions diluted in DMSO were tested at a final concentration of 10 $\mu g.mL^{-1}$ and 25 $\mu g.mL^{-1}$. A positive control REV (resveratrol, 50 µM), and solvent control, DMSO (0.1%) were included in each assay plate. On 4 DPF, the egg water and compounds were renewed, and deceased larvae were removed. The larvae were also exposed to Nile Red at a final concentration of 10 $ng.mL^{-1}$. On the last day of the bioassay, 5 DPF, larvae were anesthetized with tricaine (MS-222, 0.03%) and fluorescence intensity was quantified in a Leica DM6000 M fluorescence microscope.

Fluorescence intensity in the yolk-sac of each larva was quantified with a plugin adapted for this purpose by the imaging software ImageJ. The mean intensity fluorescence (MFI) of the fractions was normalized to the mean value of the DMSO control (100%), and the data were statistically analysed for significant differences with the control.

2.5. Statistical analysis

The data were analysed for statistical differences with the program GraphPad Prism 9. The Gaussian distribution was tested by normality tests, namely by Shapiro-Wilk and Kolmogorov-Smirnov normality tests (P value < 0.05) and for equal variances using Bartlett's test. If the Gaussian assumption was met (normal or parametric distribution) and the data had equal variance, the differences were analysed by One-Way ANOVA with Dunnett's multiple comparison test (P value < 0.05). If the Gaussian assumption was met but the data did not have equal variance, a Brown-Forsythe and Welch ANOVA with Dunnett's multiple comparison test (P value < 0.05) was applied. On the other hand, if the data had non-parametric distribution, they were transformed through square root transformation and tested again for their normality. If the Gaussian assumption was met, then the data were treated as mentioned above. If not, the differences were analysed by Kruskal-Wallis with Dunn's multiple comparison test (P value < 0.05). The data from the biochemical characterization were represented as column bars of mean with standard deviation, and significant differences among the groups were indicated by different letters. The data from the zebrafish bioassays were represented as box-whisker plots, and fractions with significance differences vs the solvent control were indicated by the symbol *.

2.6. Metabolite profiling

2.6.1. Liquid Chromatography with Tandem Mass Spectrometry (LC-MS/MS)

Samples for metabolic profiling were previously dried and then resuspended to a concentration of 1 $mg.ml^{-1}$ in acetonitrile, LC-MS grade, and syringe-filters with a diameter of 0.2 µm (Millex Syringe Filter, Merck Millipoore Millex ™, Darmstadt, Germany) into 2 ml vials (Millex Syringe Filter, Merck Millipoore Millex ™, Darmstadt, Germany). The LC/MS analysis was carried out by Orbitrap Exploris 120 Mass Spectrometer (Thermo Scientific™) coupled with a column ACE UltraCore 2.5 SuperC18 (50x2.1 mm; 5 µm ACE® UltraCore™, Aberdeen, Scotland), with electrospray ionization

(ESI) source, operating in positive mode and controlled by Xcalibur 4.4.16.14 (Thermo Scientific™). Each sample was injected with a volume of 5 µl and the samples were eluted with a gradient of 99.5% of the mobile phase A (95% H_2O + 5% MeOH + 0.1% formic acid), by decreasing mobile phase A to 10% and increasing mobile phase B to 90% at 9.5 minutes, eventually rose to 99.5% the mobile phase A and decreased to 0.5% the mobile phase B at 17 minutes. The gradient was established at a flow rate of 0.35 ml/min for 20 minutes. Separation temperature was kept at 40ºC for the entire analysis.

2.6.2. Molecular networking and metabolomic analysis

Using the MSConvert software (Proteo Wizard version 3.0.21232) the data were converted from the original RAW format to mzML format. Converted data were uploaded to the web server Global Natural Products Social Molecular Networking (GNPS) using the WinSCP software (Martin Prikryl version 5.19.2.11614). Then, molecular networks were generated in the online platform of GNPS, an open access database with the goal of sharing tandem mass spectrometry (MS/MS) data [83]. The Precursor Ion Mass Tolerance (PIMT) and Fragment Ion Mass Tolerance (FIMT) were set to 0.02 Da (high resolution equipment as qTOF or Orbitrap). The obtained results were then visualized and analysed using the software program Cytoscape (version 3.8.2).

Aiming the identification of potential known or unknown compounds responsible for the observed bioactivities, active and non-active extracts were compared. The MS/MS spectrums of the metabolites only present in the active extracts (unique metabolites) were compared to several MS/MS spectrums databases included on the GNPS platform (Dereplicator, Dereplicator + and MoINetEnhancer). At the section “Data Analysis” – “Library Search”, the PIMT and FIMT were set to 2.0 and 0.5 respectively, because a lot of data in MS/MS databases come from low-resolution equipment [80].

For hits not identified in previous databases, manual searches on other databases were performed, such as Dictionary of Marine Natural Products (DMNP, https://dmnp.chemnetbase.com) and Dictionary of Natural Products (DNP, https://dnp.chemnetbase.com). Lastly, the *m/z* error was calculated in parts per million (ppm), $\frac{m}{z} error\ (ppm) = \frac{(\frac{m}{z} peak - \frac{m}{z} data\ base) \times 10^6}{\frac{m}{z} peak}$.

3. Results

3.1. Light Experiment

With the intention to analyse how light affects the production of metabolites from the *Cyanobium* sp. LEGE 07173, several biochemical parameters were assessed for significant differences among the different light conditions (1B – middle light; 2A – strong light; 2B – continuous light; 3A – blue light; 3B – red light). Then, the cultures were extracted and fractionated, and the fractions tested for anti-obesity activity.

3.1.1. Freeze-dried biomass

The culture volume needed for biochemical characterization was harvested, and the remaining volume was centrifuged, and the pellet freeze-dried for future extraction. The freeze-dried biomasses were weighted, which allows an evaluation of culture growth. The obtained masses – 1B (36.9 mg); 2A (42.6 mg); 2B (62.1 mg); 3A (80.5 mg); 3B (38.3 mg) – were represented in $g.L^{-1}$ of culture in Fig. 3 for easier visualization.

3.1.2. Dry-biomass

Dry-biomass is a measure for cyanobacteria growth and was used as a normalizing factor. The culture exposed to condition 2B (continuous light) grew significantly more ($p < 0.05$) when compared to the other conditions. Significant growth differences ($p < 0.05$) were also found between condition 1B (middle light) and condition 3B (red light), the latter presenting higher values of dry-biomass. Cultures exposed to conditions 2A (strong light) and 3A (blue light) showed similar dry-biomass values, and no significant differences were found between these conditions and conditions 1B (middle light) and 3B (red light) (Fig. 3).

Theoretically, the obtained results for freeze-dried biomass and dry-biomass shouldn't be much different. However, condition 3A (blue-light) appears with strong growth in freeze-dried biomass, contrary to dry-biomass. This cyanobacteria has a tendency to sediment, especially under higher densities. As a result, the samples taken for dry-biomass only account for suspended biomass, as well as the samples taken for biochemical parameters. Thus, dry-biomass normalizes to the density of a determined volume taken for the evaluation of proteins, carbohydrates, lipids and pigments. Additionally, the absolute values of biomass obtained in dry-biomass are much higher than those of freeze-dried biomass. It's possible that the methodology for dry-biomass measure overestimated the actual biomass growth that occurred.

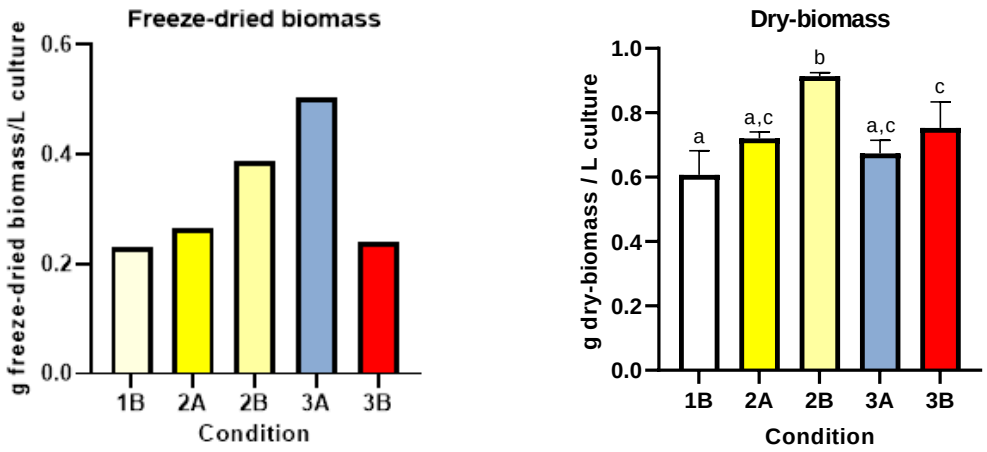

Fig. 3 – Freeze-dried biomass (left) and dry-biomass (right) obtained for each condition in the light experiment (1B – middle light; 2A – strong light; 2B – continuous light; 3A – blue light; 3B – red light). On the left, values are expressed in g freeze-dried biomass/ L culture (n = 1). On the right, values are expressed in g dry-biomass/ L culture (n = 3). Statistical differences were analysed by ordinary one-way ANOVA with Dunnett's multiple comparisons test. Significant differences are represented as different letters if ($p < 0.05$).

3.1.3. Protein Content

In condition 2B (continuous light) less protein is present compared to all other conditions, significantly ($p < 0.05$) in contrast with conditions 1B (middle light) and 3A (blue light). Conditions 2A (strong light) and 3B (red light) had similar protein content values and showed no significant differences when compared to all of the other conditions (Fig. 4).

3.1.4. Carbohydrate content

No significant differences in carbohydrate content were found among the different light conditions (Fig. 4).

3.1.5. Lipid content

In condition 2B (continuous light) less lipids are present compared to all other conditions, significantly ($p < 0.05$) in contrast with conditions 2A (strong light) and 3B (red light). However, condition 2A (strong light) also showed significant differences ($p < 0.05$) when compared to condition 1B (middle light), contrary to condition 3B (red light). Furthermore, no significant differences were found between middle light, blue light, and red light (Fig. 4).

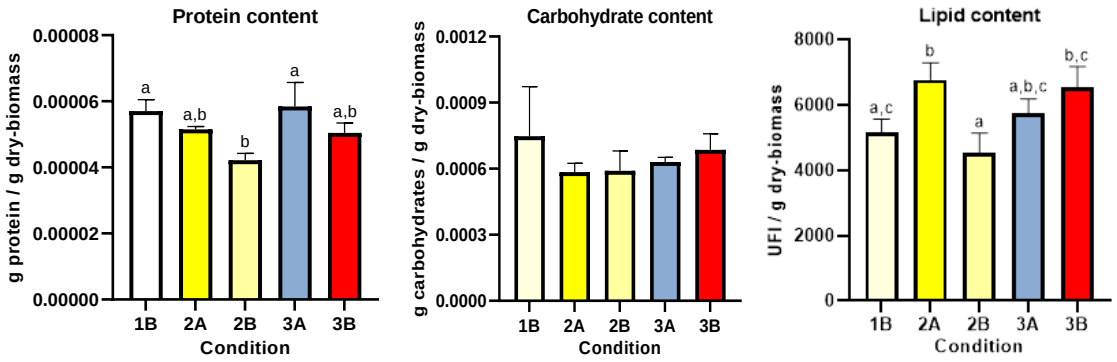

Fig. 4 – Protein (left), carbohydrate (middle) and lipid (right) content obtained for each condition in the light experiment (1B – middle light; 2A – strong light; 2B – continuous light; 3A – blue light; 3B – red light). Values are expressed in g protein/ g dry-biomass (left), g carbohydrates/ g dry-biomass (middle), and in unit of fluorescence intensity (UFI) /g dry-biomass (right) (n = 3). Statistical differences were analysed by ordinary one-way ANOVA with Dunnett's multiple comparisons test. Significant differences are represented as different letters if ($p < 0.05$).

3.1.6. Pigments

The obtained results are similar for chlorophyll a, chlorophyll b and carotenoids content. The culture exposed to continuous light (2B) showed significantly higher ($p < 0.05$) pigments content than all the other cultures. No significant differences were observed between conditions 1B (middle light) and 2A (strong light) nor between condition 2A, 3A (blue light) and 3B (red light). Condition 1B also showed significantly higher ($p < 0.05$) pigment content than condition 3A and 3B (Fig. 5).

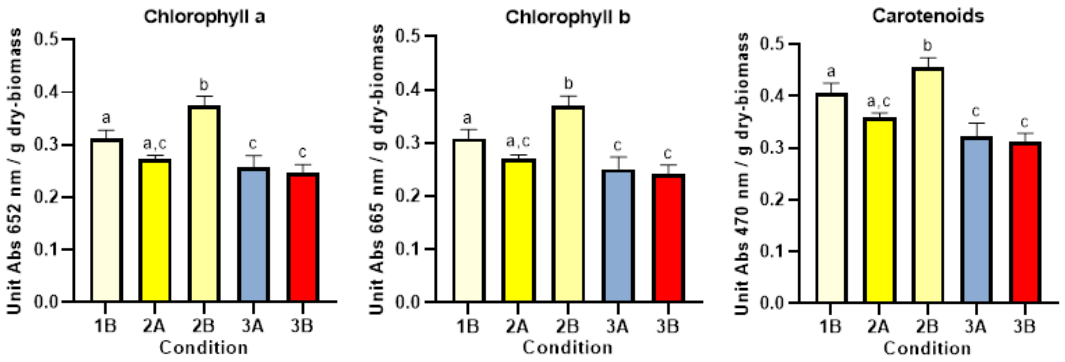

Fig. 5 – Pigment content (chlorophyll a, chlorophyll b and carotenoids) obtained for each condition in the light experiment (1B – middle light; 2A – strong light; 2B – continuous light; 3A – blue light; 3B – red light). Values are expressed in unit Abs 652 nm/ g dry-biomass for chlorophyl a, unit Abs 665 nm/ g dry-biomass for chlorophyl b and unit Abs 470 nm/ g dry-biomass for carotenoids (n = 3). Statistical differences were analysed by ordinary one-way ANOVA with Dunnett's multiple comparisons test. Significant differences are represented as different letters if ($p < 0.05$).

Overall, middle light decreased biomass production and increased protein content with no strong effects on other parameters. Strong light led to an increase in lipid production. Continuous light increased biomass and pigments but decreased protein and lipid content. Blue light induced strong growth, as well as higher protein production, however, decreased pigment content. Red light increased lipids but lead to pigment content reduction, as well as decreased growth. Finally, carbohydrate content wasn't affected by any light condition. A general overview of the results is presented in Table 1.

Table 1 – General overview of the results obtained for the biochemical characterization of the light experiment. Biomass refers to freeze-dried biomass (n = 1). Other parameters had 3 replicates. + represents increase, - represents decrease, when the different light conditions are compared.

	Parameter				
Condition	Biomass	Proteins	Carbohydrates	Lipids	Pigments
1B (middle light)		+			
2A (strong light)				+	
2B (continuous light)	+	–		–	+
3A (blue light)	+	+			–
3B (red light)				+	–

3.1.7. Zebrafish Bioassays

The fractions obtained from the cultures of the light experiment were tested for their lipid-reducing activity in a final concentration of 10 µg.mL^{-1} and 25 µg.mL^{-1} (Fig. 6). The results were analysed for significant differences relative to the solvent control (DMSO). No significant different lipid reduction was observed in any of the fractions and concentrations tested (Fig. 7), however, fraction 1B-A (middle light fraction A) at 25 µg.mL^{-1} final concentration revealed a lipid reduction percentage of 31.35 ± 21.66 (mean ± standard deviation, SD). Statistical analysis resulted in a P value of p = 0.1.

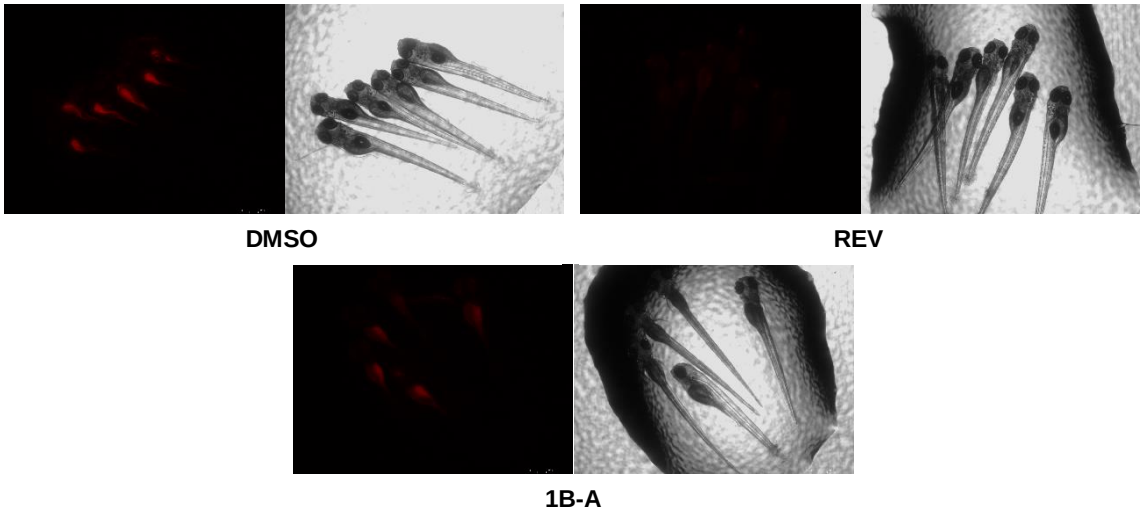

Fig. 6 – Representative images of the zebrafish Nile Red fat metabolism assay of fraction 1B-A (middle light fraction A) at 25 µg.mL^{-1} final concentration. DMSO, solvent control 0.1%; REV, positive control 50 µM.

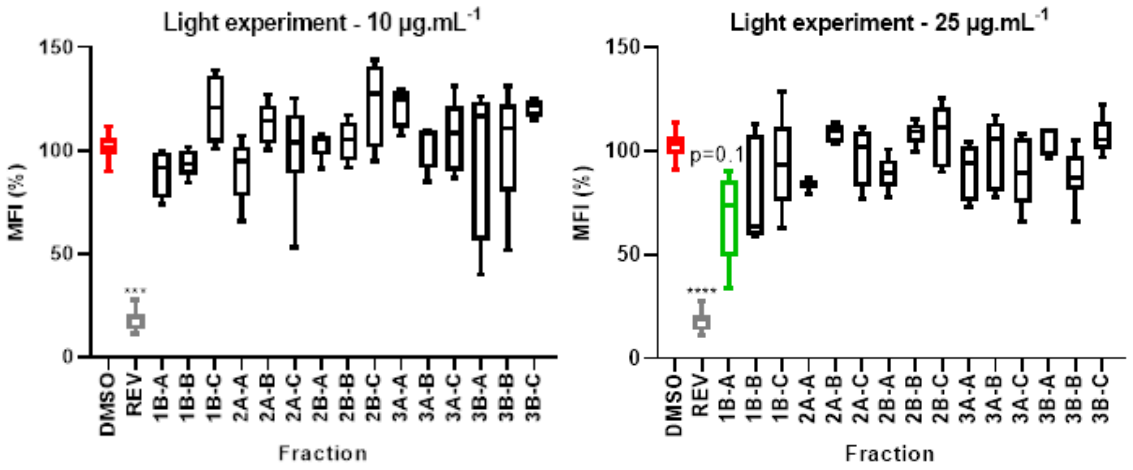

Fig. 7 – Lipid-reducing activity in the zebrafish Nile Red fat metabolism assay for light experiment fractions at 10 µg.mL^{-1} (left) and 25 µg.mL^{-1} (right). Solvent control had 0.1% DMSO and the positive control 50 µM REV. Values are expressed as mean fluorescence intensity (MFI) relative to the DMSO group, and each treatment group had 5 to 7 replicates. The data are represented as box-whisker plots. Statistical differences were analysed by Kruskal-Wallis with Dunn's multiple comparisons test and are indicated to the solvent control with the symbol * $p < 0.05$; ** $p < 0.01$; *** $p < 0.001$; **** $p < 0.0001$.

3.2. Zebrafish bioassays with BOGA culture

The observed bioactivity in the light experiment wasn't as substantial as expected and associated to high variability, compared with earlier data from the research group, where a 50% reduction was obtained at 10 µg.mL^{-1} [73]. Differences may be derived by the chosen culture conditions (light intensity) or extraction methodology (MeOH extraction). As next, the strain was analysed from the original growth conditions (cultured in the facility of CIIMAR, BOGA) and extracted with the original methodology

(DCM:MeOH extraction) and the one used in the light experiment (MeOH extraction). Fractions from the two different extraction methods were tested for their lipid reduction activity in a final concentration of 10 µg.mL^{-1} and 25 µg.mL^{-1} (Fig. 8). Interesting reductions of neutral lipids were found in fraction A of both extractions and both concentrations (Table 2). No significant bioactivity was observed in any of the fractions and concentrations tested, however, the statistical analysis resulted in P values very close to 0.05 in fraction A of the dichloromethane/methanol extraction (DM-A) in both concentrations ($p = 0.06$ in 10 µg.mL^{-1} final concentration and $p = 0.1$ in 25 µg.mL^{-1} final concentration) (Fig. 9).

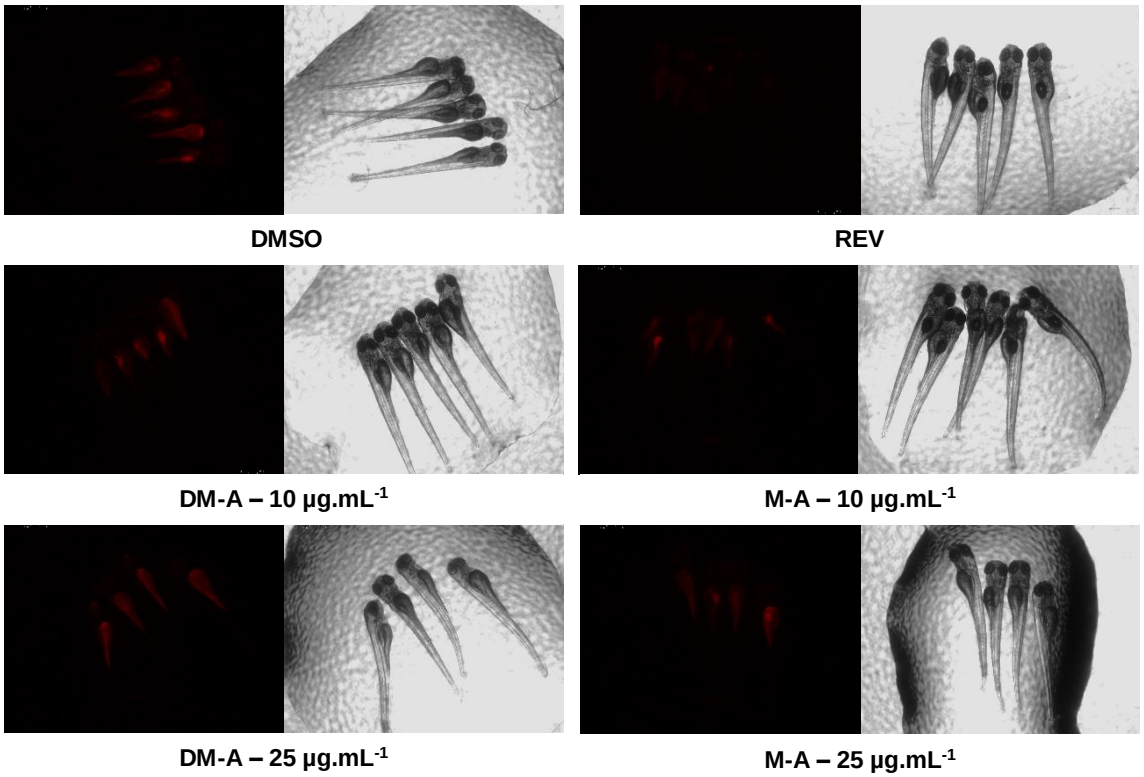

Fig. 8 – Representative images of the zebrafish Nile Red fat metabolism assay of fractions DM-A (methanol: dichloromethane extraction fraction A) and M-A (methanol extraction fraction A) at 10 µg.mL^{-1} and 25 µg.mL^{-1} final concentration. DMSO, solvent control 0.1%; REV, positive control 50 µM.

Table 2 – Lipid-reducing activity of the fractions A obtained from de BOGA cultures (mean ± standard deviation, SD).

Final concentration	Fraction	Reduction ± SD (%)
10 µg.mL^{-1}	DM-A	23.89% ± 27.42
	M-A	20.38% ± 32.95
25 µg.mL^{-1}	DM-A	35.97% ± 14.29
	M-A	30.70% ± 20.11

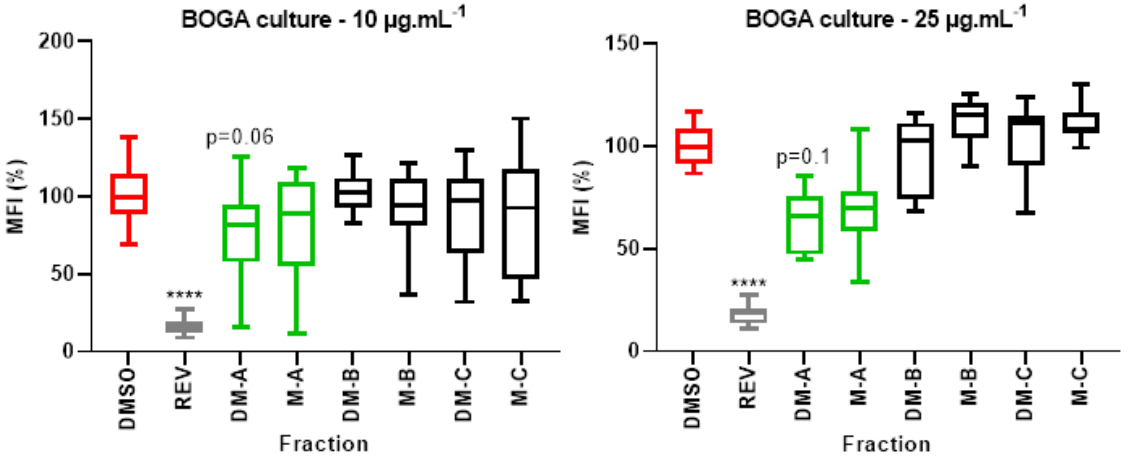

Fig. 9 – Lipid-reducing activity in the zebrafish Nile Red fat metabolism assay for BOGA culture fractions at 10 µg.mL^{-1} (left) and 25 µg.mL^{-1} (right). Solvent control had 0.1% DMSO and the positive control 50 µM REV. Values are expressed as mean fluorescence intensity (MFI) relative to the DMSO group, and each treatment group had 5 to 7 replicates. The data are represented as box-whisker plots. Statistical differences were analysed by Kruskal-Wallis with Dunn's multiple comparisons test and are indicated to the solvent control with the symbol * $p < 0.05$; ** $p < 0.01$; *** $p < 0.001$; **** $p < 0.0001$.

3.3. Temperature experiment

Aiming to understand if metabolites production is affected by temperature in this cyanobacteria, a range of temperatures (1A – 10°C; 1B – 14°C; 2A – 18°C; 2B – 22°C; 3A – 26°C; 3B – 30°C) were tested and several biochemical parameters were assessed and analysed for significant differences. Later, the cultures were extracted and fractionated, and the fractions tested for lipid-reducing activity.

3.3.1. Freeze-dried biomass

The culture volume needed for biochemical characterization was harvested, and the remaining volume was centrifuged, and the pellet freeze-dried for future extraction. The freeze-dried biomasses were weighted, which allows an evaluation of culture growth. The obtained masses – 1A (338.9 mg); 1B (448.5 mg); 2A (687.1 mg); 2B (773.7 mg); 3A (786.1 mg); 3B (700.4 mg) – were represented in g.L^{-1} of culture in Fig. 13 for easier visualization.

3.3.2. Dry-biomass

Like in the light experiment, dry-biomass was used as a normalizing factor. Cultures 2A (18°C) and 3B (30°C) showed similar dry-biomass values that were significantly higher ($p < 0.05$) than the values of the other conditions. Moreover, significant differences ($p < 0.05$) were found between the conditions 1A (10°C) and 3A (26°C). Conditions 1B (14°C) and 2B (22°C) showed similar dry-biomass values and no

significant differences were found between these conditions and conditions at 10°C and 26°C (Fig. 14).

Once again, the freeze-dried biomass and dry-biomass aren't consistent, due to sedimentation of cyanobacteria. Condition 2B (22°C) and 3A (26°C) show strong growth in the freeze-dried biomass, contrary to dry-biomass. As explained above in 3.1.2, dry-biomass normalizes to the density of a determined volume.

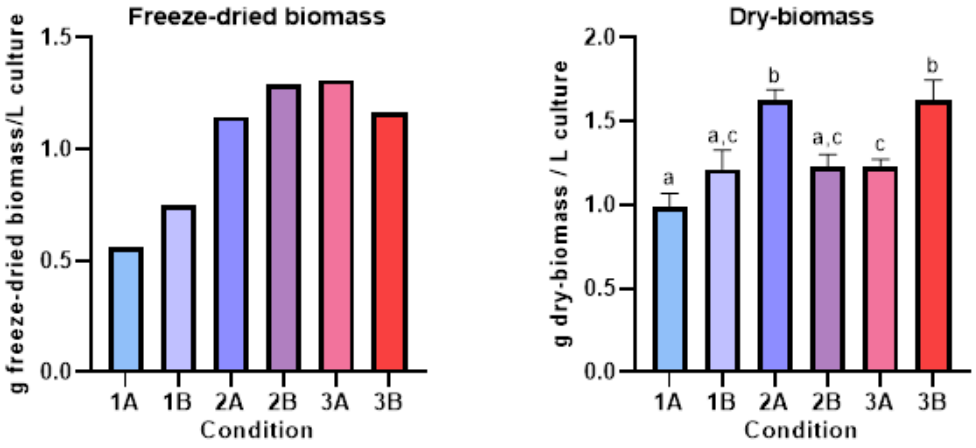

Fig. 10 – Freeze-dried biomass (left) and dry-biomass (right) obtained for each condition in the temperature experiment (1A – 10°C; 1B – 14°C; 2A – 18°C; 2B – 22°C; 3A – 26°C; 3B – 30°C). On the left, values are expressed in g freeze-dried biomass/ L culture (n = 1). The data are represented as column bars. On the right, values are expressed in g dry-biomass/ L culture (n = 3). Statistical differences were analysed by ordinary one-way ANOVA with Dunnett's multiple comparisons test. Significant differences are represented as different letters if ($p < 0.05$).

3.3.3. Protein content

Protein content was particularly high at 22°C (2B) and 30°C (3B), although only the first shows significant differences ($p < 0.05$) when compared to the lowest protein content, at 18°C (2A). No significant differences were found between conditions 1A (10°C), 1B (14°C), 3A (26°C) and 3B (30°C), nor between them and cultures at 18°C and 22°C (Fig. 11).

3.3.4. Carbohydrate content

Condition 3A (26°C) revealed a significantly higher ($p < 0.05$) carbohydrate content when compared to conditions 1A (10°C), 1B (14°C), 2A (18°C) and 2B (22°C). Condition 3B (30°C), however, showed no significant differences with any of the conditions. Also, no significant differences were found between conditions 1A, 1B, 2A and 2B (Fig. 11).

3.3.5. Lipid content

At 10°C (1A) there was significantly higher ($p < 0.05$) lipid content in comparison to all other conditions, except for condition 2B (22°C). There were no significant differences observed between the latter and conditions 1B (14°C), 2A (18°C), 3A (26°C) and 3B (30°C) (Fig. 11).

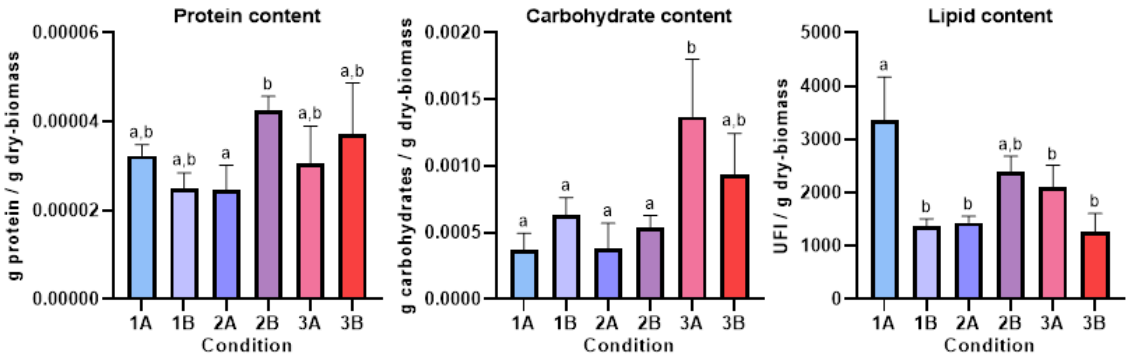

Fig. 11 – Protein (left), carbohydrate (middle) and lipid (right) content obtained for each condition in the temperature experiment (1A – 10°C; 1B – 14°C; 2A – 18°C; 2B – 22°C; 3A – 26°C; 3B – 30°C). Values are expressed in g protein/ g dry-biomass (left), g carbohydrates/ g dry-biomass (middle), and in unit of fluorescence intensity (UFI) /g dry-biomass (right) (n = 3). Statistical differences were analysed by ordinary one-way ANOVA with Dunnett's multiple comparisons test. Significant differences are represented as different letters if ($p < 0.05$).

3.3.6. Pigments

In chlorophyl a content, the condition 2B (22°C) displayed significantly higher chlorophyl a values than all other conditions ($p < 0.05$), except for condition 3A (26°C). Significant differences ($p < 0.05$) were also found at 10°C (1A) and 26°C, the latter showing higher chlorophyl a values. No significant differences were observed between conditions 1A, 1B (14°C), 2A (18°C) and 3B (30°C), nor between conditions 1B (14°C), 2A (18°C), 3A (26°C) and 3B (30°C).

In chlorophyl b content, the culture 1A (10°C) showed significantly lower ($p < 0.05$) chlorophyll b values than conditions 2B (22°C) and 3A (26°C) ($p < 0.05$), but no significant differences were found when compared with conditions 1B (14°C), 2A (18°C) and 3B (30°C). Conditions 1B (14°C), 2B (22°C) and 3A (26°C) showed no significant differences, as well as cultures at 1B (14°C), 2A (18°C), 3A (26°C) and 3B (30°C).

Finally, in carotenoids content, conditions 1B (14°C), 2B (22°C) and 3A (26°C) showed no significant differences among themselves, however, condition 2B (22°C) showed significantly higher carotenoids content ($p < 0.05$) when compared with conditions 1A (10°C), 2A (18°C) and 3B (30°C). No significant differences were found at

10°C (1A), 14°C (1B), 18°C (2A) and 30°C (3B), nor at conditions 10°C (1A), 14°C (1B), 22°C (3A) and 30°C (3B). Additionally, significant differences ($p < 0.05$) were found between condition 2A (18°C) and 3A (22°C) (Fig. 12).

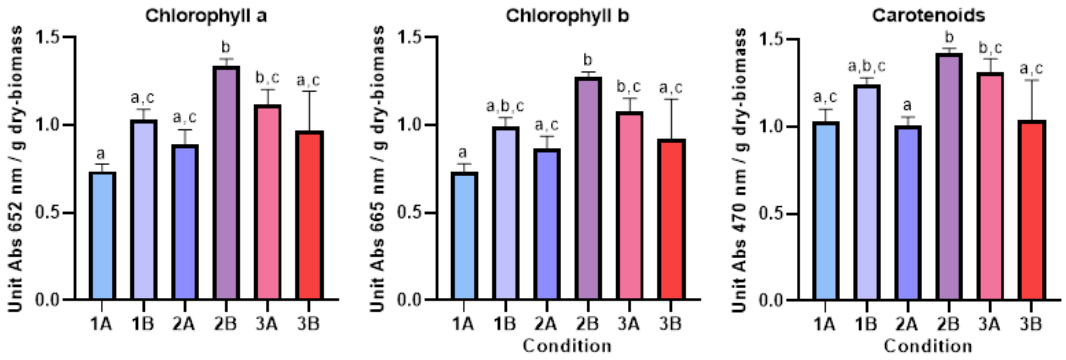

Fig. 12 – Pigment content (chlorophyll a, chlorophyll b and carotenoids) obtained for each condition the temperature experiment (1A – 10°C; 1B – 14°C; 2A – 18°C; 2B – 22°C; 3A – 26°C; 3B – 30°C). Values are expressed in unit Abs 652 nm/ g dry-biomass for chlorophyl a, unit Abs 665 nm/ g dry-biomass for chlorophyl b and unit Abs 470 nm/ g dry-biomass for carotenoids (n = 3). Statistical differences were analysed by ordinary one-way ANOVA with Dunnett's multiple comparisons test. Significant differences are represented as different letters if ($p < 0.05$).

Generally, the higher the temperature, the stronger growth, except at 30°C. At 10°C, lipid content increased dramatically. At 14°C and 18 °C no major changes in the biochemical content of the cells were found. At 22°C, protein and pigment production was induced. A remarkable increase in carbohydrate content was found at 26°C. Lastly, at 30°C, carbohydrate content also increased, but to a lesser extent. A general overview of the results is presented in Table 3.

Table 3 – General overview of the results obtained for the biochemical characterization of the temperature experiment. Biomass refers to freeze-dried biomass (n = 1). Other parameters had 3 replicates. + represents increase, - represents decrease, when the different temperature conditions are compared.

	Parameter				
Condition	Biomass	Proteins	Carbohydrates	Lipids	Pigments
1A (10°C)	–			+	
1B (14°C)	–				
2A (18°C)					
2B (22°C)	+	+			+
3A (26°C)	+		+		
3B (30°C)			+		

3.3.7. Zebrafish bioassay

The fractions produced from the cultures of the temperature experiment were tested in the zebrafish Nile Red fat metabolism assay for their anti-obesity activity at a final concentration of 25 µg.mL^{-1} (Fig. 13). The lipid reductions obtained for bioactive fractions are represented in Table 4. Significant differences relative to the solvent control ($p < 0.05$) were observed at 10°C, 14°C and 18°C in fraction A (1A-A, 1B-A and 2A-A respectively) (Fig. 14).

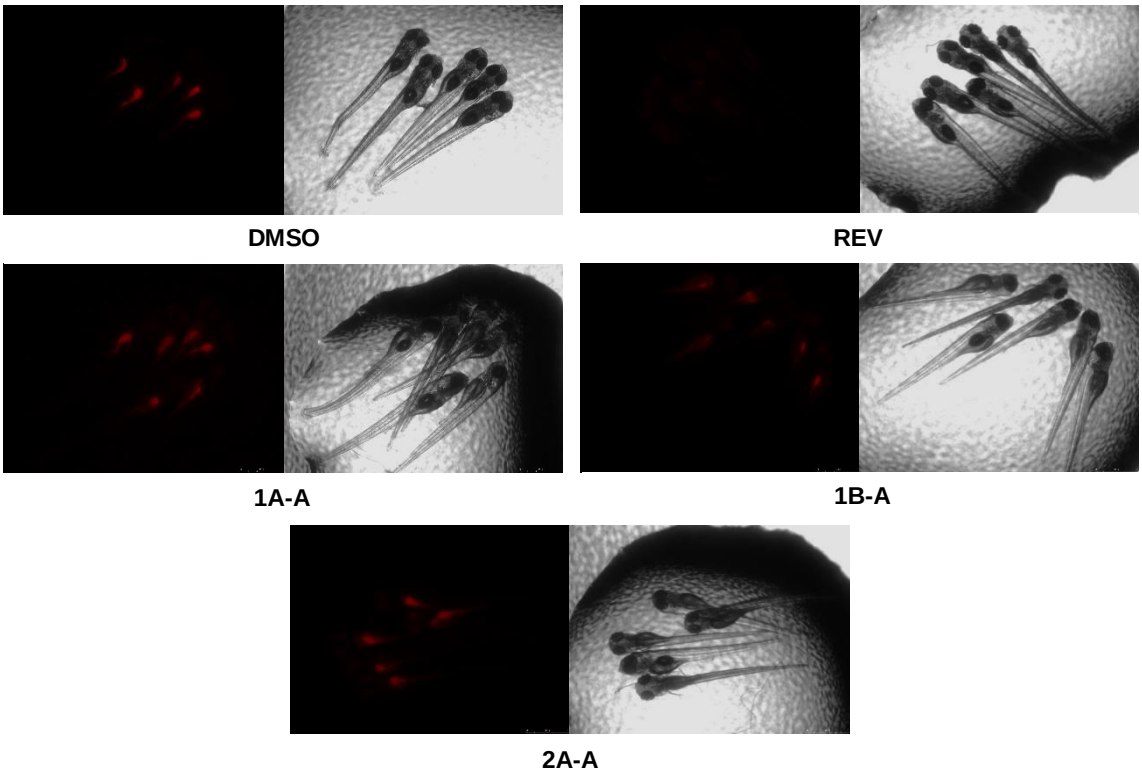

Fig. 13 – Representative images of the zebrafish Nile Red fat metabolism assay of fractions 1A-A (10°C), 1B-A (14°C) and 2A-A (18°C) of the temperature experiment at 25 µg.mL^{-1} final concentration. DMSO, solvent control 0.1%; REV, positive control 50 µM.

Table 4 – Lipid-reducing activity of the fractions A obtained from the cultures of the temperature experiment (mean ± standard deviation, SD).

Fraction	Reduction ± SD (%)
1A-A	13.64% ± 9.04
1B-A	27.60% ± 15.19
2A-A	22.06% ± 8.57

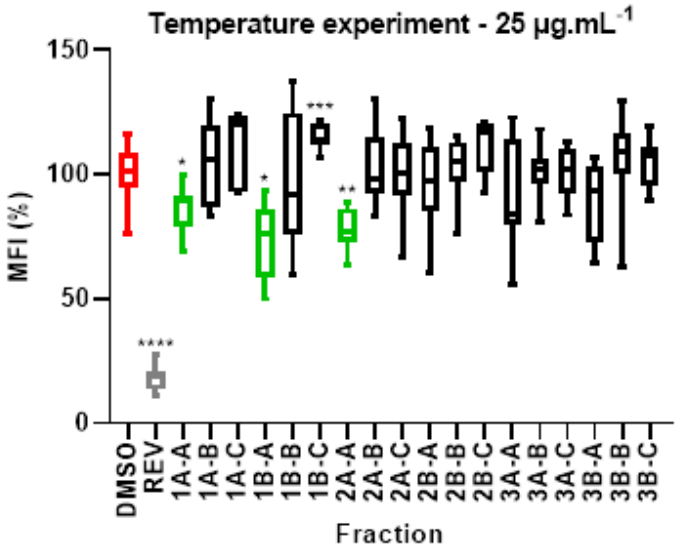

Fig. 14 – Lipid-reducing activity in the zebrafish Nile Red fat metabolism assay for temperature experiment fractions at 25 µg.mL^{-1}. Solvent control had 0.1% DMSO and the positive control 50 µM REV. Values are expressed as mean fluorescence intensity (MFI) relative to the DMSO group, and each treatment group had 5 to 7 replicates. The data are represented as box-whisker plots. Statistical differences were analysed by Brown-Forsythe and Welch ANOVA with Dunnett's multiple comparisons test and are indicated to the solvent control with the symbol * $p < 0.05$; ** $p < 0.01$; *** $p < 0.001$; **** $p < 0.0001$.

3.4. Metabolite profiling

The extracts whose fractions had the greatest potential for lipid-reducing activity were selected for analysis by LC-MS/MS aiming the discovery of possible responsible metabolites. Two extracts with bioactive fraction A (1B-A and 2A-A) as well as three extracts with non-active fractions (2B-A, 3A-A and 3B-A) from the temperature experiment were used for the comparative analysis of metabolite profiles, aiming the identification of known or unknown compounds unique to the bioactive samples. A molecular network was generated using Cytoscape through the analysis by the GNPS platform. Molecular networks are composed of nodes that represent spectrums, which can be organized by clusters (sets of nodes), representing common molecular structures. Through a colour code is possible to visualize which nodes are only present in active samples and which are present in active and non-active samples. The active extracts (1B-A and 2A-A) are represented in shades of green, non-active extracts (2B-A, 3A-A and 3B-A) are represented in shades of blue and blanks are represented in black (Fig. 15). More than 30 nodes unique for the active samples were found (Appendix II), however, only 7 of these were shared between 1B and 2A. Thus, these MS/MS spectrums simultaneously unique for both bioactive extracts were selected and searched in several databases (GNPS, DMNP and DNP). The information obtained from the databases, as well as the calculated *m/z* error in ppm, are presented in Table 5.

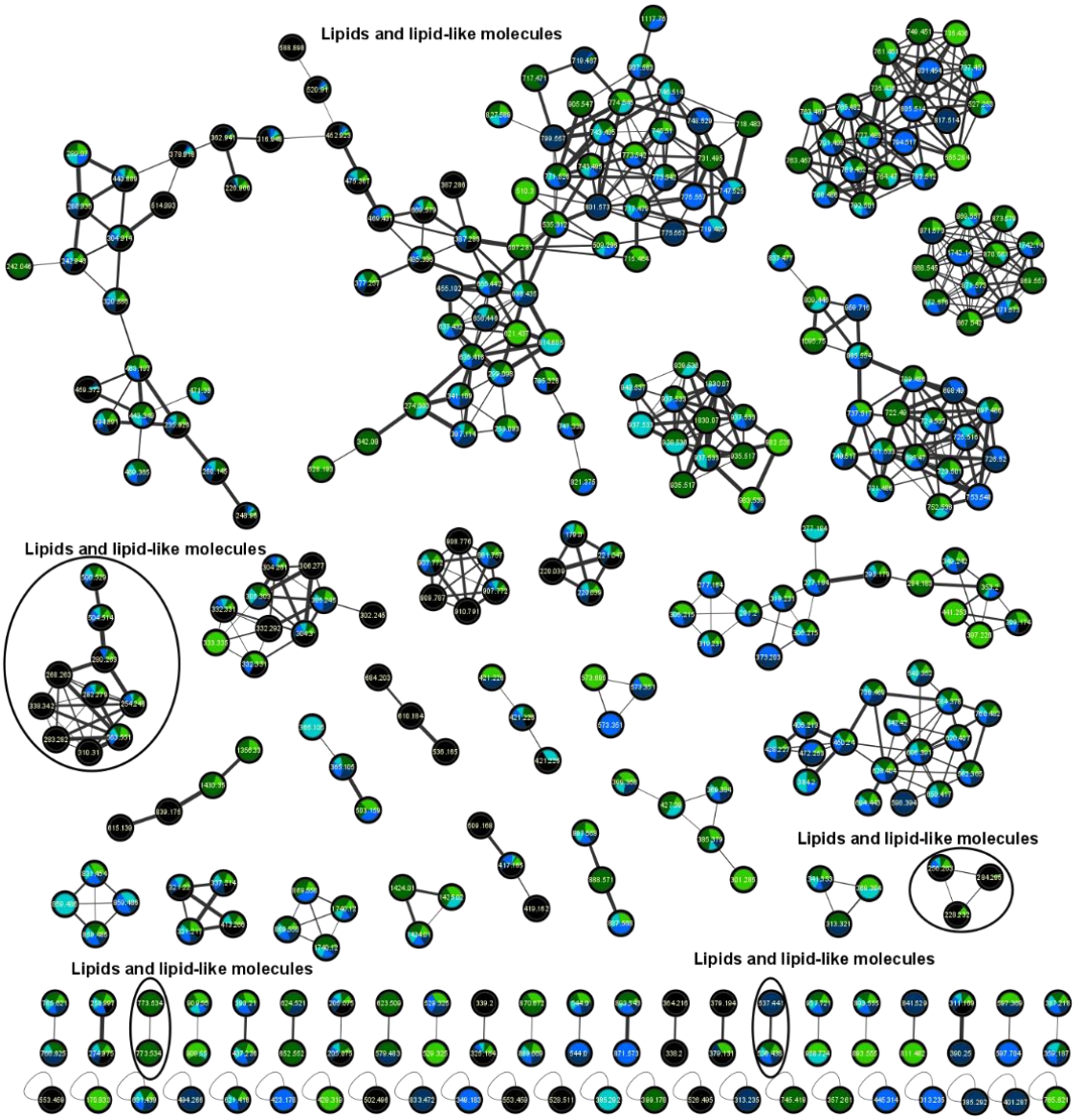

Fig. 15 – Molecular network of the temperature extracts 1B and 2A (active samples – shades of green), and 2B, 3A and 3B (non-active samples – shades of blue) obtained by the GNPS platform and visualized with Cytoscape. Blanks are represented in black.

Table 5 – Putative identification of unique mass peaks in active fractions in the Global Natural Products Social Molecular Networking (GNPS) platform, including Dereplicator and Dereplicator +, Dictionary of Marine Natural Products (DMNP), and Dictionary of Natural Products (DNP). The table shows the 7 unique mass peaks. Dereplicator identifications are based on MS/MS spectrums, while identifications for DMNP and DNP are based on the accurate mass, searched in a range of +/- 0.002. M, accurate mass; $M+H^+$, mass + hydrogen (parent mass); RT, retention time; ppm, parts per million.

$M+H^+$	RT	Putative Identification	*m/z* error (ppm)	Formula	Source
294.183	732.873	Not identified			
507.281	567.692	Cyclomarin A 13,14-Deepoxy,13,14-didehydro, N50-de-Me			Dereplicator
528.193	35.471	Dapiramicin B	-2.26	$C_{21}H_{29}N_5O_{11}$	DNP
715.464	746.610	Cholestane-3,6,15,24-tetrol; (3β,5α,6α,15α,24S)-form, 3-O-(2-O-Methyl-β-D-xylopyranoside), 24-O-α-L-arabinofuranoside	1.04	$C_{38}H_{66}O_{12}$	DMNP
		Mytilus Inhibitory peptides; MIP-6	2.93	$C_{35}H_{58}N_{10}O_6$	
867.542	851.246	Virotoxin [Ala1] Viroidin			Dereplicator
1356.330	923.264	Not identified			
1430.350	941.772	Petriellin A			Dereplicator

4. Discussion

Cyanobacteria are capable of incredible environment adaptation, being able to change their metabolism pathways in order to produce secondary metabolites that allow them to survive and grow in stress situations [43]. These metabolites are often bioactive and have potential application in the treatment of many diseases, namely metabolic diseases, such as obesity [45]. Together with secondary metabolites, the concentration of other components of cyanobacterial cells, such as proteins, carbohydrates, lipids and pigments, will also change with this adaptation [58]. Thus, modifications in the biochemical composition of the cells are an indicator of altered metabolism [57, 59]. Discovering the optimal conditions which render improved accumulation of target metabolites without biomass loss is of major importance to turn natural products with pharmaceutical application economically competitive [54].

As photoautotrophic organisms, cyanobacteria need a light source to obtain energy and convert it to chemical energy like ATP and NADP [55]. Light quantity and quality affect cell metabolism and therefore modulate biomass composition [56, 81]. Furthermore, photoperiod regulates cell division, which occurs during light period, and it is accelerated under continuous illumination conditions [56]. Nevertheless, oxygenic photosynthesis leads to photodamage of PSII. Since photosynthetic electron flow starts from the reduction of plastoquinone by electrons released by oxidation of water at PSII, the accumulation of photodamaged PSII decreases photosynthetic activity [60]. When the rate of photodamage surpasses the rate of PSII repair, photoinhibition follows, and when severe, can lead to growth decline and cell death [61]. Photoinhibition commonly happens under environmental stress conditions [60]. As such, when microalgal cells are subjected to high light intensities or other forms of stress, the excess electrons in photosynthetic electron transport chain induce the generation of numerous ROS, thereby causing the inhibition of photosynthesis, pigment co-oxidation, lipid peroxidation, membrane destruction and protein denaturation [62]. To mitigate the effects of oxidative stress in cells, cyanobacteria may produce lipids or carbohydrates, that can serve as receptors to dissipate excess electrons. Which type of energy-producing compound will accumulate in the microalgal cell appears to be species-specific [84].

LEGE 07173 was exposed to a range of light intensities, namely 150 µmol $m^{-2}s^{-1}$ (middle light), 500 µmol $m^{-2}s^{-1}$ (strong light) and 150 µmol $m^{-2}s^{-1}$ 24 hours day (continuous light). The biomass growth was much higher under continuous light. A study using *Scenedesmus obliquus*, in which the microalgae was exposed to 150 µmol $m^{-2}s^{-1}$ of white

light under a photoperiod of 24 hours day and 12 hours day:12 hours night, revealed that continuous conditions of light led to high biomass concentration, in addition to decreased lipid production [85]. In fact, the same tendency was observed in this work, being continuous light the condition with the lowest lipid content. However, in *Scenedesmus*, continuous light decreased chlorophyll content and no differences were found in protein content between conditions [85]. LEGE 07173 revealed high chlorophyll and carotenoid content, while protein production decreased under continuous light. Still, a decrease in chlorophyl a with high light exposure is consistent with the nature of this pigment. On one hand, two key enzymes involved in biological synthesis of chlorophyll a, glutamyl-tRNA reductase (GluTR), and glutamate 1-semialdehyde aminotransferase (GSA-AT) are sensitive to light and their activity could be inhibited by excessive light exposure. On the other hand, the molecule itself is unstable and easily broken under higher light intensity [86]. Moreover, under optimum cultivation conditions, cyanobacteria generally tend to produce more proteins in order to maintain cell multiplication and biomass production [87]. The low protein content under continuous light may indicate that cells were no longer under optimal conditions and the high exposure to light was starting to cause photodamage and consequent cell growth stagnation. Chlorophyll was accumulated during optimal growth and was not yet affected by this process by the time the experiment ended.

In this work, both chlorophyll a and b were measured, however, it's important to note that the existence of chlorophyll b among cyanobacteria is extremely rare and only few of these organisms are generally accepted as chlorophyl b synthetising cyanobacteria (for instance, marine cyanobacteria belonging to the *Prochlorococcus* genus) [88]. The very similar results for chlorophyll a and b obtained in every condition in both light and temperature experiments, suggest that chlorophyll a may be absorbing at both wavelengths 652.4 nm and 665.2 nm, and chlorophyll b likely does not exist.

The growth under strong light was only slightly higher than the verified under middle light. Furthermore, strong light induced lipid production which suggests that the cells were under stress [84]. In a study developed by Guyon at al., *Ostreococcus* strain OTTH595 showed simillar growth when exposed to a light intensity of 150 µmol $m^{-2}s^{-1}$ and 500 µmol $m^{-2}s^{-1}$ [89]. In a research work using *Chlorella* sp. and *Monoraphidium dybowskii*, microalgae were exposed to 40, 200 and 400 µmol $m^{-2}s^{-1}$ of light intensity. The highest light intensity led to fast growth in the first few days, but was eventually surpassed by the intermediate light intensity, likely due to photoinhibition. Like in the present work, an increase of lipid content was observed with increased light intensity [62].

Moreover, blue light potentiated strong growth. Blue light was shown to stimulate biomass growth in different microalgae species. A study carried out by Teo et al. demonstrated that *Nannochloropsis* sp. and *Tetraselmis* sp., two marine microalgae, grew better under blue light rather than red light [90]. Another study conducted by Duarte at al. using *Synechococcus* sp. revealed that blue LEDs increased the growth of the cyanobacteria by 80%, compared to previous studies. In addition, blue light didn't accentuate lipid production [82]. These results are similar to the ones we observe in the present study – because blue light did not cause cell stress, lipid production isn't stimulated, and protein content increases to maintain biomass growth [84, 87]. Conversely, red light induced lipid accumulation and little cyanobacteria growth, similarly to strong light, thus indicating that the cells were under stress [84]. Surprisingly, both conditions led to a decrease in pigment content. While this was expected in red light, since photoinhibition may cause pigment co-oxidation [62], the same shouldn't happen under optimal conditions, such as, apparently, blue light. The fact that blue light induced a much faster growth compared to the other conditions might be a possible explanation, since pigment accumulation could not be promoted [91].

Overall, strong light and red light appear to cause stress in *Cyanobium sp.* 07173, mostly due to increased lipid production and low biomass growth. Blue light emerges as an optimal condition for robust growth. Lastly, continuous light also induced strong growth, however, the clear decreased protein content may suggest photoinhibition. Middle light was the condition with closest similarity to the conditions in BOGA, and revealed high protein production, which indicates that cyanobacteria weren't under stress, and cellular functions were working normally. If the goal was to produce high quantity of biomass, then blue light would be the obvious choice. However, our objective was to optimize culture conditions for the production of metabolites with anti-obesity properties.

The zebrafish Nile Red fat metabolism assay using the fractions obtained from the light experiment revealed a reduction in neutral lipids of about 30% only in fraction A from middle light conditions at 25 $\mu g.mL^{-1}$ final concentration. As such, is possible to assume, based on the particular conditions that were tested, that the production of yet unknown metabolites responsible for the lipid-reducing activity isn't modulated under light-stress conditions, nor under optimal growth conditions of light. The lipid-reducing activity obtained for fraction A of middle light condition was highly variable (± 21.66 % SD) and not significantly different from the control, in contrast to previous screenings, which revealed a lipid reduction of 50% at 10 $\mu g.mL^{-1}$ final concentration [73]. The light conditions themselves could be affecting metabolite production; even though middle light

conditions were similar to BOGA conditions, there were some important disparities, namely light intensity (150 µmol $m^{-2}s^{-1}$ vs 80 – 125 µmol $m^{-2}s^{-1}$) and temperature (25°C vs 20°C). Furthermore, the light experiment cultures were extracted using methanol (M). The original extraction methodology applied in the initial screening was dichloromethane:methanol (DM). Thus, cultures extracted using different methodologies were compared in the zebrafish bioassay, and this might have affected the results.

Following, cultures from the bioterium of CIIMAR (BOGA) were extracted with both methodologies. Results revealed that the extraction methodology didn't have a substantial impact in the bioactivities, in contrast to our expectations. At 10 µg.mL^{-1} final concentration, dichloromethane:methanol fraction A (DM-A) and methanol fraction A (M-A) showed similar lipid-reducing activity, about 20% with high SDs associated. At 25 µg.mL^{-1} final concentration, the bioactivities were 35.97 ± 14.29 % (mean ± SD) for DM-A and 30.70 ± 20,11 % (mean ± SD) for M-A. Therefore, lipid-reducing capacity was similar in both extraction methodologies, however, did not reach statistical significance. In addition, the results obtained using the dichloromethane:methanol extraction were slightly improved and less variable, so this extraction method was chosen for the cultures of the temperature experiment.

Temperature is one of the most important factors in microalgae cultivation and its highly correlated with growth rate [84]. Temperature influences metabolic processes and cell composition, as well as cell size and nutrient requirements. Temperature tolerance range and optimal growth temperature vary from strain to strain [92]. Generally, cyanobacteria growth increases with higher temperatures, until a threshold is reached [84]. At supra-optimal conditions of temperature, protein degradation is induced leading to cell mortality. Additionally, temperature stress strongly affects ROS dynamics, causing progressive oxidative damage and ultimately cell death [93].

LEGE 07173 was exposed to a range of temperatures, namely 10°C, 14°C, 18°C, 22°C, 26°C and 30°C. As expected, biomass production increased gradually with temperature. At 30°C a decrease in biomass production was observed, indicating that optimal growth temperature had already been exceeded. Cell growth was similar and particularly high at 22°C and 26°C, suggesting that the optimal growth temperature for this cyanobacteria is around this range. A study conducted by Ranglová et al., in which several microalgae species were exposed to temperatures from 15°C to 35°C revealed that *Scenedesmus almeriensis* and *Chlorella* R-117 had optimal growth at 25°C [94]. Another study, where microalgae were exposed to the same range of temperatures,

demonstrated that *Nannochloropsis oculata* also had higher growth rate at 25°C, and total lipid accumulation was increased at 30°C [95].

Several distinct descriptions of how temperature affects lipid accumulation have been reported. For instance, *Synechocystis* sp. PCC6803 demonstrated optimal growth at 30-33°C and serious lipid production inhibition at 18°C, 22°C and 40°C [96]. *Scenedesmus* sp. LX1 showed optimal biomass and lipid production at 20°C [97]. *Spirulina platensis* exposed to mediums of different nitrogen concentration and 3 temperatures (15°C, 25°C and 35°C) revealed higher lipid content in the lowest temperature in all nitrogen concentrations [98]. These conflicting data demonstrate that temperature impact on lipid production is highly species-specific. Besides, the mechanism underling lipid accumulation remains unclear [95]. However, is generally accepted that lipid proportions change under stress situations [57, 84]. Under optimal growth conditions, fatty acids are synthesized primarily for esterification into glycerol-based membrane lipids. Conversely, under an unfavourable environment for growth, lipid biosynthetic pathways are altered towards the formation and accumulation of neutral lipids in the form of triacylglycerol (TAG), as a type of storage of carbon and energy [99]. In the present study, there was a clear increased production of lipids at 10°C, which is consistent with an enhanced accumulation of neutral lipids under stressful conditions.

On the contrary, high temperatures (26°C and 30°C) induced carbohydrate synthesis. This suggests a shift in the metabolic pathways for carbon storage in the cell when temperature increases and exceeds optimal temperature growth. It has been proposed that carbohydrate and lipid synthesis are two competing pathways, mainly in studies regarding nitrogen depletion [100-102]. However, in a study led by Chokshi et al. it was demonstrated that microalgae *Acutodesmus dimorphus* exposed to 25°C, 35°C and 38°C, gradually increased carbohydrate production and decreased lipid accumulation with increasing temperature, further confirming the relationship between lipid and carbohydrate production under stress [103]. In LEGE 07173, it seems that the preferred pathway for carbon storage is temperature dependent – low temperature induces lipid production and high temperature leads to carbohydrate accumulation.

The results obtained in the biochemical characterization of the temperature experiment reveal that under the temperature of 14°C and over the temperature of 22°C, the cyanobacteria starts to generate stress responses, namely by dramatically increasing lipid production at 10°C and carbohydrate synthesis over 26°C. Moreover, the high biomass growth, protein and pigment content at 22°C suggest that, from all the temperatures tested, this is the one who stimulates the best biomass yield without stress

induction [62, 87, 93]. Considering that BOGA cultures were at 20°C, the closest conditions in this experiment were the cultures kept at 18°C and 22°C. Still, the light intensity was different: 80 – 125 µmol $m^{-2}s^{-1}$ in BOGA and 150 µmol $m^{-2}s^{-1}$ in the photobioreactors, as well as the control of pH level in the reactors.

The fractions of the temperature experiment were tested in the zebrafish Nile Red fat metabolism assay, and fraction A from the cultures at 10°C, 14°C and 18°C revealed significant lipid-reducing activity in comparison to the DMSO control ($p < 0.05$). While the bioactivity between the fractions of the conditions at 14°C and 18°C were similar – 27.60 ± 15.19% and 22.06 ± 8.57% (mean ± SD), respectively – the activity observed with fraction A at 10°C condition was much lower – 13.64 ± 9.04% (mean ± SD). Thus, is presumable that the stress caused by low temperature, namely the activation of pathways for increased lipid production, affected the syntheses of responsible metabolites. Furthermore, no bioactivity was found at temperatures higher than 22°C. Like in the light experiment, the conditions that displayed strong biomass growth (continuous light, blue light, 22°C, 26°C and 30°C) lost bioactive potential. Then, it is possible to infer that the activation of pathways for increased cellular growth led to a reduction or inactivation of the metabolic pathways for production of anti-obesity compounds. Finally, the bioactivities obtained over the course of this work are less strong than the previously reported 50% lipid reduction at 10 µg.mL^{-1} [76]. More rehearsals are needed to understand these inconsistencies and truly comprehend the role of culture conditions on the anti-obesity potential of this cyanobacteria.

In this work, fractions from several different light and temperature conditions to which the cyanobacteria *Cyanobium* sp. LEGE 07173 was exposed, were tested for lipid-reducing activity. In the bioassay for the temperature experiment, three fractions (1A-A, 1B-A and 2A-A) demonstrated statistically significant lipid reduction, being fractions 1B-A and 2A-A the ones with stronger reduction. As such, the extracts from conditions 1B (14°C) and 2A (18°C) were selected for metabolite profiling, together with the extracts from conditions 2B (22°C), 3A (26°C) and 3B (30°C) that did not show lipid reduction activity. The comparison between metabolite profiles of active and non-active extracts allowed the discovery of MS/MS spectrums only present in the active extracts (unique metabolites), which were putatively identified by searching in several mass spectrometry databases. Considering the information collected by the databases and the calculation of *m/z* error, several compounds were suggested as unique metabolites in both fractions with anti-obesity activity in the zebrafish bioassays, and hence, potentially involved in this bioactivity. The smaller the difference between the mass peak in the database and in the molecular network data (*m/z* error closest to 0), the higher is the probability of the

mass peak matching that compound. From the 7 selected MS/MS mass peaks, it was possible to identify 5, almost all with previously described bioactivities. Both non-identified mass peaks could represent novel molecules, since no match in any database was found.

The mass peak [M+H$^+$] 507.281 was putatively identified as cyclomarin A in the GNPS platform included database Dereplicator (identifications based on MS/MS spectrums). This compound is a cyclic heptapeptide, firstly isolated from *Streptomyces* sp., with anti-malarian activity that inhibits the growth of blood stage *Plasmodium falciparum* with an IC_{50} value of 40 nM [104]. It was also shown to have anti-tubercular action, being bactericidal against *Mycobacterium tuberculosis*, including resistant strains, in human-derived macrophages in a concentration of 2.5 nM [105]. When it was first isolated, moderate activity toward tumour cell lines was also reported [106]. Furthermore, cyclomarin A has been licensed to Phytera Inc for therapeutic use as a potent anti-inflammatory and anti-viral agent (Pazoles and Siegel, US patent 5759995A) [107]. Chronic inflammation of adipose tissue is closely associated with metabolic disorders such as obesity due to pathologic alterations of white adipose tissue metabolism and pro-inflammatory bias of secreted adipokines, which have systemic effects on the organism health status [108]. Activation of inflammatory signalling pathways, such as TLR4-mediated activation of Mitogen-activated protein kinases (MAPKs) and nuclear factor-kappa B (NF-κB), is considered to be a relevant link between obesity and related comorbidities such as cancer, diabetes and cardiovascular disease [109]. Thus, anti-inflammatory agents may have inhibitory effects on adipose tissue differentiation. For instance, the anti-inflammatory marine cyclic heptapeptide, stylissatin A was shown to inhibit the differentiation of murine 3T3-L1 preadipocytes (EC_{50} = 9.1 and 1.9 μM), proving that specific inflammatory signalling pathways might be supressed to inhibit adipogenesis and/or activate lipogenesis [109]. Microcystin LR, is an example of a well-known cyclic heptapeptide, isolated from the freshwater cyanobacterium *Microcystis aeruginosa* [110]. Nonetheless, no reports have been found on the isolation of cyclomarin A from cyanobacteria.

The mass peak [M+H$^+$] 528.193 was identified as dapiramicin B through the DNP database with a *m/z* error of -2.26 ppm (based on similarity of *m/z* value). Dapiramicin B is a nucleoside antibiotic isolated from *Micromonospora* sp. SF-1917, active against sheath blight in rice plants, but much less effective than related antibiotic dapiramicin A [111]. Nucleoside antibiotics are a large family of microbial natural products derived from nucleosides and nucleotides. Because nucleosides and nucleotides play essential roles in cellular metabolism, nucleoside antibiotics exhibit a broad spectrum of bioactivities,

such as anti-bacterial, anti-fungal, anti-viral, anti-tumour, insecticidal, immunostimulant and immunosuppressive activity [112]. Two nucleoside derivatives, 3-acetyl-2′-deoxyuridine and 3-phenylethyl-2′-deoxyuridine, were isolated from the marine cyanobacterium *Moorea producens*, both of which showed moderate activity towards the MCF-7 cancer cell line with IC_{50} values of 18.2 μM and 22.8 μM, respectively [113].

Two compounds were identified through the DMNP platform for the same mass peak [$M+H^+$] 715.464. Cholestane, synonym granulatoside B, is a steroidal glycoside isolated from the starfish *Choriaster granulatus* [114]. Although other granulatosides revealed immunomodulatory activity in murine peritoneal macrophages, no bioactivity was reported on this compound [115]. Several structurally diverse steroidal glycosides have been isolated from different microalgae, such as *Chaetoceros calcitrans*, *Phaeodactylum tricornutum* and *Haslea ostrearia* [116]. The calculated *m/z* error of this compound is 1.04 ppm. Mytilus Inhibitory Peptide 6 (MIP-6) is a muscle contractor inhibitor isolated from the adductor muscle of the bivalve mollusc *Mytilus edulis* [117]. The anticoagulant activity of the protein hydrolysate from the adductor muscle of *M. edulis* was evaluated by molecular docking and Peptide Ranker and results showed that IC_{50} value was 1.49 $mg.mL^{-1}$ [118]. The calculated *m/z* error of this compound is 2.93 ppm. Given the *m/z* errors of these compounds, is more likely that the mass peak corresponds to granulatoside B, or to a compound of simillar structure.

The mass peak [$M+H^+$] 867.542 was putatively identified by the GNPS platform included database Dereplicator (identifications based on MS/MS spectrums). Petriellin A, a cyclic depsipeptide isolated from organic extracts of an antagonistic coprophilous fungus, *Petriella sordida*, that has shown antifungal activity against *Ascobolus furfuraceous* and *Sordaria funicula* in a concentration of 5 $\mu g.mL^{-1}$ [119, 120]. Other cyclic depsipeptides have been noted for their anti-obesity potential. For instance, aurilide is a potent inhibitor of mitochondrial prohibitin 1 [121]. The inhibition of prohibitin 1 was shown to induce apoptosis in the vasculature of white adipose tissue, leading to fat resorption and normalization of metabolism, resulting in obesity reversal in mice [122]. Thus, aurilide, like other similar molecules, is a potential compound of interest in obesity treatment [123]. Several structurally analogous aurilides have been isolated from different cyanobacterial species, for instance, *Lyngbya majuscula* [124]. Viequeamide A is another cyclic depsipeptide isolated from marine cyanobacterium *Rivularia* sp. [125]. However, no reports have been found on the isolation of petriellin A from cyanobacteria or microalgae.

Finally, mass peak [$M+H^+$] 1430.350 was identified by the GNPS platform included database Dereplicator (identifications based on MS/MS spectrums) as virotoxin [Ala1] viroidin, a cyclic peptide toxin isolated from *Amanita virosa* mushrooms, toxic in a range of 1 – 5 $mg.kg^{-1}$ in mice [126]. Extracts from *A. virosa* revealed strong anti-bacterial activity effects against *Staphylococcus aureus* [127]. Peptide natural products arising from ribosomal pathways are referred to as ribosomally synthesized and post-translationally modified peptides, or RiPPs. Virotoxins are cycloamanides, macrocyclic RiPPs produced by fungi [128]. Macrocyclic RiPPs produced by cyanobacteria are called cyanobactins, and biosynthetic genes for their production have been described in distantly related cyanobacteria *Prochloron*, *Trichodesmium*, *Microcystis*, *Nostoc*, *Lyngbya*, and *Anabaena* [129]. However, no reports have been found on the production of virotoxins by cyanobacteria or microalgae.

Overall, most of the metabolites were putatively identified as cyclic peptides, namely cyclomarin A, petriellin A and virotoxin [Ala1] viroidin. Cyclic peptides are compounds of particular interest in pharmacological application due to their chemical diversity, potent bioactivities, low toxicity, good binding affinity, and target selectivity, and several of these metabolites were selected for clinical trials, mainly for cancer treatment, such as soblidotin, aplidine and bryostatin 1. Furthermore, vancomycin is already clinically used as an antibiotic to treat various bacterial infections [130, 131]. Many of these compounds display bioactivities towards a number of different human diseases. For instance, the identified cyclomarin A exhibits anti-malarian, anti-tubercular, anti-viral, anti-cancer and anti-inflammatory activities [104-107]. The above mentioned stylissatin A is an anti-inflammatory and inhibits adipocyte differentiation [109]. Given the diverse role of prohibitin 1 in disease pathogenesis, aurilide has therapeutic potential against cancer, inflammation, diabetes and obesity [123]. (−)-Ternatin, a cyclic heptapeptide isolated from mushroom *Coriolus versicolor*, was shown to suppress hyperglycaemia in KK-Ay mice at 17 nmol final concentration [132], and to inhibit HCT116 cancer cell proliferation (IC_{50} = 71 nM) [133]. Thus, even though none of the identified metabolites had previously described anti-obesity properties, is possible that one or more are responsible for the lipid-reducing activity observed in the zebrafish bioassays. However, further experiments are needed to validate these results. In particular, further efforts are needed to strengthen the putative identifications. MS2 fragmentation pattern should be compared between experimental mass peaks and putative matches from databases if such information is present in the scientific literature. Alternatively, *in silico* predictions of main fragmentations could be manually compared to experimental MS/MS fragments.

5. Conclusion

The main goal of this work was to manipulate the growth conditions of *Cyanobium* sp. LEGE 07173, a cyanobacteria with previously reported lipid-reducing activity, in order to identify and optimize the production of responsible secondary metabolites. The effects of light and temperature conditions were analysed through various biochemical parameters, and the bioactivity of the fractions were tested in the zebrafish Nile Red fat metabolism assay. Furthermore, metabolite profiling allowed the identification of potential compounds, which might be involved in the anti-obesity activity.

The biochemical analysis proved that light and temperature conditions affected the metabolism of the cyanobacteria, given the different values of protein, carbohydrate, lipid and pigment content, as well as biomass growth obtained. Blue light and continuous light promote strong cell growth, as well as temperatures above 22°C. However, in the zebrafish bioassays, it was notable that conditions promoting biomass growth, did not induce bioactivity. At the same time, stress conditions, such as strong light, red light and high temperature (26°C and 30°C) also caused loss of activity. These results suggest that the responsible metabolites are synthetized under neither stress nor optimal growth conditions, but are stimulated under certain conditions, which need to be evaluated experimentally. Growth at temperatures of 10°C, 14°C and 18°C under middle light conditions (150 µmol $m^{-2}s^{-1}$) and with extractions by DCM:MeOH followed by fractionation with hexane (A fraction, nonpolar compounds) revealed the anti-obesity activity present in the cyanobacterial strain LEGE 07173.

These experimental results allowed the generation of a metabolite network focusing on the comparison between active and non-active samples (A fractions) in order to identify unique compounds in the active samples. Such metabolite profiling revealed 7 potential responsible metabolites, where 5 putative identifications have still a certain degree of uncertainty, and 2 mass peaks may represent novel molecules. Most of these compounds had previously described bioactivities. Particularly, 3 cyclic peptides were identified – cyclomarin A, petriellin A and virotoxin [Ala1] viroidin. Cyclic peptides are interesting molecules from a pharmacological point of view, and many display bioactivities towards a number of different human diseases. As such, even though none of the identified metabolites had previously described anti-obesity properties, they may be responsible for the lipid-reducing activity observed in the zebrafish bioassays. However, further experiments are needed to validate these results.

6. References

1. WHO. *Obesity and Overweight*. 2021; Available from: https://www.who.int/news-room/fact-sheets/detail/obesity-and-overweight.
2. Alman, K.L., et al., *Dietetic management of obesity and severe obesity in children and adolescents: A scoping review of guidelines.* Obesity Reviews, 2021. **22**(1): p. e13132.
3. Oliveira, A., et al., *Prevalence of general and abdominal obesity in Portugal: Comprehensive results from the National Food, nutrition and physical activity survey 2015–2016.* BMC Public Health, 2018. **18**(1): p. 1-9.
4. Huppertz, C., *Anti-obesity Drugs.* Encyclopedia of Molecular Pharmacology, 2020: p. 1-6.
5. Zang, L., L.A. Maddison, and W. Chen, *Zebrafish as a model for obesity and diabetes.* Frontiers in cell and developmental biology, 2018. **6**: p. 91.
6. Urbatzka, R., et al., *Lipid reducing activity and toxicity profiles of a library of polyphenol derivatives.* European Journal of Medicinal Chemistry, 2018. **151**: p. 272-284.
7. Rodríguez-Pérez, C., A. Segura-Carretero, and M. del Mar Contreras, *Phenolic compounds as natural and multifunctional anti-obesity agents: A review.* Critical Reviews in Food Science and Nutrition, 2019. **59**(8): p. 1212-1229.
8. Jiang, S.Z., et al., *Obesity and hypertension.* Experimental and Therapeutic Medicine, 2016. **12**(4): p. 2395-2399.
9. Djalalinia, S., et al., *Health impacts of obesity.* Pakistan Journal of Medical Sciences, 2015. **31**(1): p. 239.
10. Apovian, C.M., *Obesity: definition, comorbidities, causes, and burden.* American Journal of Managed Care, 2016. **22**(7 Suppl): p. s176-85.
11. Chu, D.-T., et al., *An update on physical health and economic consequences of overweight and obesity.* Diabetes & Metabolic Syndrome: Clinical Research & Reviews, 2018. **12**(6): p. 1095-1100.
12. Tremmel, M., et al., *Economic burden of obesity: a systematic literature review.* International Journal of Environmental Research and Public Health, 2017. **14**(4): p. 435.
13. Engin, A., *The definition and prevalence of obesity and metabolic syndrome.* Obesity and lipotoxicity. Advances in Experimental Medicine and Biology, 2017. **964**: p. 1-17.

14. Apovian, C.M., *The obesity epidemic—understanding the disease and the treatment*. New England Journal of Medicine, 2016. **374**(2): p. 177-179.
15. Jakobsen, G.S., et al., *Association of bariatric surgery vs medical obesity treatment with long-term medical complications and obesity-related comorbidities.* Jama, 2018. **319**(3): p. 291-301.
16. Nguyen, N.T. and J.E. Varela, *Bariatric surgery for obesity and metabolic disorders: state of the art.* Nature Reviews. Gastroenterology & Hepatology, 2017. **14**(3): p. 160-169.
17. Balaji, M., et al., *A review on possible therapeutic targets to contain obesity: The role of phytochemicals.* Obesity Research & Clinical Practice, 2016. **10**(4): p. 363-380.
18. Tak, Y.J. and S.Y. Lee, *Anti-obesity drugs: long-term efficacy and safety: an updated review.* The World Journal of Men's Health, 2021. **39**(2): p. 208.
19. Castro, M., et al., *Obesity: The metabolic disease, advances on drug discovery and natural product research.* Current Topics in Medicinal Chemistry, 2016. **16**(23): p. 2577-2604.
20. Chan, Y., et al., *Natural products in the management of obesity: Fundamental mechanisms and pharmacotherapy.* South African Journal of Botany, 2021. **143**: p. 176-197.
21. Sridhar, S., et al., *Natural products-based pancreatic lipase inhibitors for obesity treatment.* Natural Bio-active Compounds, 2019. Springer. p. 149-191.
22. Noinart, J., et al., *A new ergosterol analog, a new bis-anthraquinone and anti-obesity activity of anthraquinones from the marine sponge-associated fungus Talaromyces stipitatus KUFA 0207.* Marine Drugs, 2017. **15**(5): p. 139.
23. Hu, X., et al., *Marine-derived bioactive compounds with anti-obesity effect: A review.* Journal of Functional Foods, 2016. **21**: p. 372-387.
24. Cardoso, S.M., et al., *Seaweeds as preventive agents for cardiovascular diseases: From nutrients to functional foods.* Marine Drugs, 2015. **13**(11): p. 6838-6865.
25. Miyashita, K. and M. Hosokawa, *Fucoxanthin in the management of obesity and its related disorders.* Journal of Functional Foods, 2017. **36**: p. 195-202.
26. Sun, X., et al., *Modulation of gut microbiota by fucoxanthin during alleviation of obesity in high-fat diet-fed mice.* Journal of Agricultural and Food Chemistry, 2020. **68**(18): p. 5118-5128.
27. Bae, M., et al., *Health benefits of fucoxanthin in the prevention of chronic diseases.* Biochimica et Biophysica Acta (BBA)-Molecular and Cell Biology of Lipids, 2020. **1865**(11): p. 158618.

28. Osório, C., et al., *Pigments content (chlorophylls, fucoxanthin and phycobiliproteins) of different commercial dried algae.* Separations, 2020. **7**(2): p. 33.
29. Seca, A.M. and D.C. Pinto, *Overview on the antihypertensive and anti-obesity effects of secondary metabolites from seaweeds.* Marine Drugs, 2018. **16**(7): p. 237.
30. Kang, S.-I., et al., *Fucoxanthin exerts differing effects on 3T3-L1 cells according to differentiation stage and inhibits glucose uptake in mature adipocytes.* Biochemical and Biophysical Research Communications, 2011. **409**(4): p. 769-774.
31. Maeda, H., *Nutraceutical effects of fucoxanthin for obesity and diabetes therapy: a review.* Journal of Oleo Science, 2015. **64**(2): p. 125-132.
32. Yim, M.-J., et al., *Suppressive effects of amarouciaxanthin A on 3T3-L1 adipocyte differentiation through down-regulation of PPARγ and C/EBPα mRNA expression.* Journal of Agricultural and Food Chemistry, 2011. **59**(5): p. 1646-1652.
33. Kim, K.-J. and B.-Y. Lee, *Fucoidan from the sporophyll of Undaria pinnatifida suppresses adipocyte differentiation by inhibition of inflammation-related cytokines in 3T3-L1 cells.* Nutrition Research, 2012. **32**(6): p. 439-447.
34. Wang, L., et al., *Fucoidan antagonizes diet-induced obesity and inflammation in mice.* Journal of Biomedical Research, 2021. **35**(3): p. 197.
35. Jin, Q., H. Yu, and P. Li, *The evaluation and utilization of marine-derived bioactive compounds with anti-obesity effect.* Current Medicinal Chemistry, 2018. **25**(7): p. 861-878.
36. Xing, M., et al., *Advances in research on the bioactivity of alginate oligosaccharides.* Marine Drugs, 2020. **18**(3): p. 144.
37. Georg Jensen, M., et al., *efficacy of alginate supplementation in relation to appetite regulation and metabolic risk factors: evidence from animal and human studies.* Obesity Reviews, 2013. **14**(2): p. 129-144.
38. Kang, M.-C., et al., *Popular edible seaweed, Gelidium amansii prevents against diet-induced obesity.* Food and Chemical Toxicology, 2016. **90**: p. 181-187.
39. Yang, T.-H., et al., *The anti-obesity effect of polysaccharide-rich red algae (Gelidium amansii) hot-water extracts in high-fat diet-induced obese hamsters.* Marine Drugs, 2019. **17**(9): p. 532.
40. Gómez-Zorita, S., et al., *Anti-obesity effects of macroalgae.* Nutrients, 2020. **12**(8): p. 2378.

41. Sharma, B.R., et al., *Caulerpa okamurae extract inhibits adipogenesis in 3T3-L1 adipocytes and prevents high-fat diet–induced obesity in C57BL/6 mice.* Nutrition Research, 2017. **47**: p. 44-52.
42. Brito, A., et al., *Culture-dependent characterization of cyanobacterial diversity in the intertidal zones of the Portuguese coast: a polyphasic study.* Systematic and Applied Microbiology, 2012. **35**(2): p. 110-119.
43. Mazard, S., et al., *Tiny microbes with a big impact: the role of cyanobacteria and their metabolites in shaping our future.* Marine Drugs, 2016. **14**(5): p. 97.
44. Pagels, F., et al., *Phycobiliproteins from cyanobacteria: Chemistry and biotechnological applications.* Biotechnology Advances, 2019. **37**(3): p. 422-443.
45. Brito, A., et al., *Bioprospecting Portuguese Atlantic coast cyanobacteria for bioactive secondary metabolites reveals untapped chemodiversity.* Algal Research, 2015. **9**: p. 218-226.
46. Vijayakumar, S. and M. Menakha, *Pharmaceutical applications of cyanobacteria—A review.* Journal of Acute Medicine, 2015. **5**(1): p. 15-23.
47. Nakata, H., et al., *Evaluation of the ameliorative effect of Spirulina (Arthrospira platensis) supplementation on parameters relating to lead poisoning and obesity in C57BL/6J mice.* Journal of Functional Foods, 2021. **77**: p. 104344.
48. Freitas, S., et al., *Chlorophyll derivatives from marine cyanobacteria with lipid-reducing activities.* Marine Drugs, 2019. **17**(4): p. 229.
49. Zhao, B., et al., *Anti-obesity effects of Spirulina platensis protein hydrolysate by modulating brain-liver axis in high-fat diet fed mice.* PloS One, 2019. **14**(6): p. e0218543.
50. Moradi, S., et al., *Effects of Spirulina supplementation on obesity: A systematic review and meta-analysis of randomized clinical trials.* Complementary Therapies in Medicine, 2019. **47**: p. 102211.
51. Bellver, M., et al., *Inhibition of Intestinal Lipid Absorption by Cyanobacterial Strains in Zebrafish Larvae.* Marine Drugs, 2021. **19**(3): p. 161.
52. Koyama, T., et al., *Anti-obesity activities of the yoshinone A and the related marine γ-pyrone compounds.* The Journal of Antibiotics, 2016. **69**(4): p. 348-351.
53. Markou, G. and E. Nerantzis, *Microalgae for high-value compounds and biofuels production: a review with focus on cultivation under stress conditions.* Biotechnology Advances, 2013. **31**(8): p. 1532-1542.
54. Kim, D.G., et al., *Manipulation of light wavelength at appropriate growth stage to enhance biomass productivity and fatty acid methyl ester yield using Chlorella vulgaris.* Bioresource Technology, 2014. **159**: p. 240-248.

55. Choi, Y.-K., et al., *LED light stress induced biomass and fatty acid production in microalgal biosystem, Acutodesmus obliquus.* Spectrochimica Acta Part A: Molecular and Biomolecular Spectroscopy, 2015. **145**: p. 245-253.
56. Sánchez-Bayo, A., et al., *Cultivation of microalgae and cyanobacteria: effect of operating conditions on growth and biomass composition.* Molecules, 2020. **25**(12): p. 2834.
57. Chen, B., et al., *Manipulating environmental stresses and stress tolerance of microalgae for enhanced production of lipids and value-added products–a review.* Bioresource Technology, 2017. **244**: p. 1198-1206.
58. Encarnação, T., et al., *Cyanobacteria and microalgae: a renewable source of bioactive compounds and other chemicals.* Science Progress, 2015. **98**(2): p. 145-168.
59. Paliwal, C., et al., *Abiotic stresses as tools for metabolites in microalgae.* Bioresource Technology, 2017. **244**: p. 1216-1226.
60. Zavafer, A., et al., *Photodamage to the oxygen evolving complex of photosystem II by visible light.* Scientific Reports, 2015. **5**(1): p. 16363.
61. Komenda, J., R. Sobotka, and P.J. Nixon, *Assembling and maintaining the photosystem II complex in chloroplasts and cyanobacteria.* Current Opinion in Plant Biology, 2012. **15**(3): p. 245-251.
62. He, Q., et al., *Effect of light intensity on physiological changes, carbon allocation and neutral lipid accumulation in oleaginous microalgae.* Bioresource Technology, 2015. **191**: p. 219-228.
63. Cave, E. and N.J. Crowther, *The Use of 3T3-L1 Murine Preadipocytes as a Model of Adipogenesis*, in *Pre-Clinical Models: Techniques and Protocols*. P.C. Guest Editor. 2019, Springer New York. p. 263-272.
64. Giacomotto, J. and L. Ségalat, *High-throughput screening and small animal models, where are we?* British Journal of Pharmacology, 2010. **160**(2): p. 204-216.
65. Benchoula, K., et al., *The promise of zebrafish as a model of metabolic syndrome.* Experimental Animals, 2019: p. 18-0168.
66. Shen, P., Y. Yue, and Y. Park, *A living model for obesity and aging research: Caenorhabditis elegans.* Critical Reviews in Food Science and Nutrition, 2018. **58**(5): p. 741-754.
67. Musselman, L.P. and R.P. Kühnlein, *Drosophila as a model to study obesity and metabolic disease.* Journal of Experimental Biology, 2018. **221**(Suppl_1): p. jeb163881.

68. Tabassum, N., et al., *Fishing for nature's hits: establishment of the zebrafish as a model for screening antidiabetic natural products.* Evidence-Based Complementary and Alternative Medicine, 2015. **2015**.
69. Warr, C.G., et al., *Using Mouse and Drosophila Models to Investigate the Mechanistic Links between Diet, Obesity, Type II Diabetes, and Cancer.* International Journal of Molecular Sciences, 2018. **19**(12): p. 4110.
70. Oka, T., et al., *Diet-induced obesity in zebrafish shares common pathophysiological pathways with mammalian obesity.* BMC Physiology, 2010. **10**(1): p. 1-13.
71. Lessman, C.A., *The developing zebrafish (Danio rerio): A vertebrate model for high-throughput screening of chemical libraries.* Birth Defects Research Part C: Embryo Today: Reviews, 2011. **93**(3): p. 268-280.
72. Jones, K.S., et al., *A high throughput live transparent animal bioassay to identify non-toxic small molecules or genes that regulate vertebrate fat metabolism for obesity drug development.* Nutrition & Metabolism, 2008. **5**(1): p. 1-11.
73. Nguyen, M., et al., *Developing 'integrative'zebrafish models of behavioral and metabolic disorders.* Behavioural Brain Research, 2013. **256**: p. 172-187.
74. Gut, P., et al., *Little fish, big data: zebrafish as a model for cardiovascular and metabolic disease.* Physiological Reviews, 2017. **97**(3): p. 889-938.
75. Tingaud-Sequeira, A., N. Ouadah, and P.J. Babin, *Zebrafish obesogenic test: a tool for screening molecules that target adiposity.* Journal of Lipid Research, 2011. **52**(9): p. 1765-1772.
76. Costa, M., et al., *Identification of cyanobacterial strains with potential for the treatment of obesity-related co-morbidities by bioactivity, toxicity evaluation and metabolite profiling.* Marine Drugs, 2019. **17**(5): p. 280.
77. Ramos, V., et al., *Cyanobacterial diversity held in microbial biological resource centers as a biotechnological asset: the case study of the newly established LEGE culture collection.* Journal of Applied Phycology, 2018. **30**(3): p. 1437-1451.
78. Kotai, J., *Instructions for preparation of modified nutrient solution Z8 for algae.* Norwegian Institute for Water Research, Oslo, 1972. **11**(69): p. 5.
79. Bradford, M.M., *A rapid and sensitive method for the quantitation of microgram quantities of protein utilizing the principle of protein-dye binding.* Analytical Biochemistry, 1976. **72**(1-2): p. 248-254.
80. Papadopoulos, K.P., et al., *Two-step treatment of brewery wastewater using electrocoagulation and cyanobacteria-based cultivation.* Journal of Environmental Management, 2020. **265**: p. 110543.

81. Alboresi, A., et al., *Light remodels lipid biosynthesis in Nannochloropsis gaditana by modulating carbon partitioning between organelles.* Plant Physiology, 2016. **171**(4): p. 2468-2482.
82. Duarte, J.H. and J.A.V. Costa, *Blue light emitting diodes (LEDs) as an energy source in Chlorella fusca and Synechococcus nidulans cultures.* Bioresource Technology, 2018. **247**: p. 1242-1245.
83. Wang, M., et al., *Sharing and community curation of mass spectrometry data with Global Natural Products Social Molecular Networking.* Nature Biotechnology, 2016. **34**(8): p. 828-837.
84. Ho, S.-H., et al., *Perspectives on engineering strategies for improving biofuel production from microalgae—a critical review.* Biotechnology Advances, 2014. **32**(8): p. 1448-1459.
85. Vendruscolo, R.G., et al., *Scenedesmus obliquus metabolomics: effect of photoperiods and cell growth phases.* Bioprocess and Biosystems Engineering, 2019. **42**(5): p. 727-739.
86. Ma, C., et al., *Cell growth and lipid accumulation of a microalgal mutant Scenedesmus sp. Z-4 by combining light/dark cycle with temperature variation.* Biotechnology for Biofuels, 2017. **10**(1): p. 260.
87. da Fontoura Prates, D., et al., *Spirulina cultivated under different light emitting diodes: Enhanced cell growth and phycocyanin production.* Bioresource Technology, 2018. **256**: p. 38-43.
88. Tanaka, R. and A. Tanaka, *Chlorophyll cycle regulates the construction and destruction of the light-harvesting complexes.* Biochimica et Biophysica Acta (BBA)-Bioenergetics, 2011. **1807**(8): p. 968-976.
89. Guyon, J.-B., et al., *Comparative Analysis of Culture Conditions for the Optimization of Carotenoid Production in Several Strains of the Picoeukaryote Ostreococcus.* Marine Drugs, 2018. **16**(3): p. 76.
90. Teo, C.L., et al., *Enhancing growth and lipid production of marine microalgae for biodiesel production via the use of different LED wavelengths.* Bioresource Technology, 2014. **162**: p. 38-44.
91. Seyfabadi, J., Z. Ramezanpour, and Z.A. Khoeyi, *Protein, fatty acid, and pigment content of Chlorella vulgaris under different light regimes.* Journal of Applied Phycology, 2011. **23**(4): p. 721-726.
92. Pagels, F., et al., *Factorial optimization of upstream process for Cyanobium sp. pigments production.* Journal of Applied Phycology, 2020. **32**(6): p. 3861-3872.
93. Serra-Maia, R., et al., *Influence of temperature on Chlorella vulgaris growth and mortality rates in a photobioreactor.* Algal Research, 2016. **18**: p. 352-359.

94. Ranglová, K., et al., *Rapid screening test to estimate temperature optima for microalgae growth using photosynthesis activity measurements.* Folia Microbiologica, 2019. **64**(5): p. 615-625.
95. Wei, L., X. Huang, and Z. Huang, *Temperature effects on lipid properties of microalgae Tetraselmis subcordiformis and Nannochloropsis oculata as biofuel resources.* Chinese Journal of Oceanology and Limnology, 2015. **33**(1): p. 99-106.
96. Sheng, J., et al., *Effects of temperature shifts on growth rate and lipid characteristics of Synechocystis sp. PCC6803 in a bench-top photobioreactor.* Bioresource Technology, 2011. **102**(24): p. 11218-11225.
97. Xin, L., H. Hong-Ying, and Z. Yu-Ping, *Growth and lipid accumulation properties of a freshwater microalga Scenedesmus sp. under different cultivation temperature.* Bioresource Technology, 2011. **102**(3): p. 3098-3102.
98. Can, S.S., E. Koru, and S. Cirik, *Effect of temperature and nitrogen concentration on the growth and lipid content of Spirulina platensis and biodiesel production.* Aquaculture International, 2017. **25**(4): p. 1485-1493.
99. Roleda, M.Y., et al., *Effects of temperature and nutrient regimes on biomass and lipid production by six oleaginous microalgae in batch culture employing a two-phase cultivation strategy.* Bioresource Technology, 2013. **129**: p. 439-449.
100. Fan, J., et al., *Oil accumulation is controlled by carbon precursor supply for fatty acid synthesis in Chlamydomonas reinhardtii.* Plant and Cell Physiology, 2012. **53**(8): p. 1380-1390.
101. Pancha, I., et al., *Nitrogen stress triggered biochemical and morphological changes in the microalgae Scenedesmus sp. CCNM 1077.* Bioresource Technology, 2014. **156**: p. 146-154.
102. Li, T., et al., *Regulation of starch and lipid accumulation in a microalga Chlorella sorokiniana.* Bioresource Technology, 2015. **180**: p. 250-257.
103. Chokshi, K., et al., *Biofuel potential of the newly isolated microalgae Acutodesmus dimorphus under temperature induced oxidative stress conditions.* Bioresource Technology, 2015. **180**: p. 162-171.
104. Bürstner, N., et al., *Gift from nature: Cyclomarin A kills mycobacteria and malaria parasites by distinct modes of action.* ChemBioChem, 2015. **16**(17): p. 2433-2436.
105. Schmitt, E.K., et al., *The natural product cyclomarin kills Mycobacterium tuberculosis by targeting the ClpC1 subunit of the caseinolytic protease.* Angewandte Chemie, 2011. **123**(26): p. 6011-6013.

106. Barbie, P. and U. Kazmaier, *Total synthesis of cyclomarins A, C and D, marine cyclic peptides with interesting anti-tuberculosis and anti-malaria activities.* Organic & Biomolecular Chemistry, 2016. **14**(25): p. 6036-6054.
107. Dadar, M., et al., *Antiinflammatory peptides: current knowledge and promising prospects.* Inflammation Research, 2019. **68**(2): p. 125-145.
108. Jayarathne, S., et al., *Anti-inflammatory and anti-obesity properties of food bioactive components: effects on adipose tissue.* Preventive Nutrition and Food Science, 2017. **22**(4): p. 251.
109. Zhang, M., et al., *Anti-inflammatory marine cyclic peptide stylissatin A and its derivatives inhibit differentiation of murine preadipocytes.* Chemical Communications, 2019. **55**(38): p. 5471-5474.
110. Gogineni, V. and M.T. Hamann, *Marine natural product peptides with therapeutic potential: Chemistry, biosynthesis, and pharmacology.* Biochimica et biophysica acta. General Subjects, 2018. **1862**(1): p. 81-196.
111. Chida, N., *Total Synthesis of Nucleoside Antibiotics Possessing Novel N-Glycoside Structures.* Journal of Synthetic Organic Chemistry, Japan, 2008. **66**(11): p. 1105-1115.
112. Niu, G. and H. Tan, *Nucleoside antibiotics: biosynthesis, regulation, and biotechnology.* Trends in Microbiology, 2015. **23**(2): p. 110-119.
113. Li, K., et al., *Glycosylated Natural Products From Marine Microbes.* Frontiers in Chemistry, 2020. **7**(879).
114. Pizza, C., et al., *Starfish saponins: 27. Steroidal glycosides from the starfish Choriaster granulatus.* Gazzetta Chimica Italiana, 1985. **115**: p. 585-589.
115. Ivanchina, N.V., et al., *Granulatosides D, E and other polar steroid compounds from the starfish Choriaster granulatus. Their immunomodulatory activity and cytotoxicity.* Natural Product Research, 2019. **33**(18): p. 2623-2630.
116. Stonik, V.A. and I.V. Stonik, *Sterol and Sphingoid Glycoconjugates from Microalgae.* Marine Drugs, 2018. **16**(12): p. 514.
117. Fujisawa, Y., et al., *Further identification of bioactive peptides in the anterior byssus retractor muscle of Mytilus: two contractile and three inhibitory peptides.* Comparative Biochemistry and Physiology Part C: Pharmacology, Toxicology and Endocrinology, 1993. **106**(1): p. 261-267.
118. Qiao, M., et al., *Identification and In Silico Prediction of Anticoagulant Peptides from the Enzymatic Hydrolysates of Mytilus edulis Proteins.* International Journal of Molecular Sciences, 2018. **19**(7): p. 2100.

119. Lee, K.K., et al., *Petriellin A: a novel antifungal depsipeptide from the coprophilous fungus Petriella sordida.* The Journal of Organic Chemistry, 1995. **60**(17): p. 5384-5385.
120. Sleebs, M.M., et al., *Total synthesis of the antifungal depsipeptide petriellin A.* The Journal of Organic Chemistry, 2011. **76**(16): p. 6686-6693.
121. Sato, S.-i., et al., *Marine natural product aurilide activates the OPA1-mediated apoptosis by binding to prohibitin.* Chemistry & biology, 2011. **18**(1): p. 131-139.
122. Kolonin, M.G., et al., *Reversal of obesity by targeted ablation of adipose tissue.* Nature Medicine, 2004. **10**(6): p. 625-632.
123. Tan, L.T., *Pharmaceutical agents from filamentous marine cyanobacteria.* Drug Discovery Today, 2013. **18**(17-18): p. 863-871.
124. Michon, S., F. Cavelier, and X.J. Salom-Roig, *Synthesis and Biological Activities of Cyclodepsipeptides of Aurilide Family from Marine Origin.* Marine Drugs, 2021. **19**(2): p. 55.
125. Wang, D., et al., *Total Synthesis of the Marine Cyclic Depsipeptide Viequeamide A.* Journal of Natural Products, 2013. **76**(5): p. 974-978.
126. Walton, J., *Chemistry of the Amanita peptide toxins*, in *The Cyclic Peptide Toxins of Amanita and Other Poisonous Mushrooms*. 2018, Springer. p. 19-57.
127. Janeš, D., et al., *Antibacterial activity in higher fungi (mushrooms) and endophytic fungi from Slovenia.* Pharmaceutical Biology, 2007. **45**(9): p. 700-706.
128. Vogt, E. and M. Künzler, *Discovery of novel fungal RiPP biosynthetic pathways and their application for the development of peptide therapeutics.* Applied Microbiology and Biotechnology, 2019. **103**(14): p. 5567-5581.
129. Sivonen, K., et al., *Cyanobactins—ribosomal cyclic peptides produced by cyanobacteria.* Applied Microbiology and Biotechnology, 2010. **86**(5): p. 1213-1225.
130. Lee, Y., C. Phat, and S.-C. Hong, *Structural diversity of marine cyclic peptides and their molecular mechanisms for anticancer, antibacterial, antifungal, and other clinical applications.* Peptides, 2017. **95**: p. 94-105.
131. Abdalla, M.A. and L.J. McGaw, *Natural cyclic peptides as an attractive modality for therapeutics: a mini review.* Molecules, 2018. **23**(8): p. 2080.
132. Kobayashi, M., et al., *Ternatin, a cyclic peptide isolated from mushroom, and its derivative suppress hyperglycemia and hepatic fatty acid synthesis in spontaneously diabetic KK-A(y) mice.* Biochemical Biophysical Research Communications, 2012. **427**(2): p. 299-304.
133. Carelli, J.D., et al., *Ternatin and improved synthetic variants kill cancer cells by targeting the elongation factor-1A ternary complex.* Elife, 2015. **4**.

Appendixes

Appendix I – Macro and micronutrients composition of Z8 medium

Table A.I 1 – Stock solution of Z8 medium.

Stock solutions	Concentration
Solution A	10 $mL.L^{-1}$
Solution B	10 $mL.L^{-1}$
Fe-EDTA solution	10 $mL.L^{-1}$
Micronutrients solution	1 $mL.L^{-1}$

Table A.I 2 – Composition of stock solution A.

Solution A		
Reagent	Name	$g.L^{-1}$
$NaNO_3$	Sodium nitrate	46.7
$Ca(NO_3)_2.4H_2O$	Calcium nitrate tetrahydrate	5.9
$MgSO_4.7H_2O$	Magnesium sulfate heptahydrate	2.5

Table A.I 3 – Composition of stock solution B.

Solution B		
Reagent	Name	$g.L^{-1}$
K_2HPO_4	Potassium phosphate dibasic	6.2
Na_2CO_3	Sodium carbonate	4.2

Table A.I 4 – Composition of stock Fe-EDTA solution.

Fe-EDTA Solution		
Solution	Name	$mL.L^{-1}$
$FeCl_3$*	Iron (III) chloride	10
EDTA-Na**	Sodium EDTA	9.5

Table A.I 5 – Composition of $FeCl_3$ solution.

***$FeCl_3$ Solution**		
Reagent	Name	100 mL
$FeCl_3.6H_2O$	Ferric chloride	2.8 g
HCl (0.1 N)	Hydrochloric acid	100 mL

Table A.I 6 – Composition of EDTA-Na solution.

****EDTA-Na Solution**		
Reagent	Name	100 mL
EDTA	Ethylenediamine tetraaceit acid	3.9 g
NaOH (0.1 N)	Sodium hydroxide solution	100 mL

Table A.I 7 – Composition of micronutrients solution.

Micronutrients Solution	
Solution	$mL.L^{-1}$
1 a 12	10
13 e 14	100

Micronutrients 1 - 14		
Reagent		$g.L^{-1}$
1	$Na_2WO4.2H_2O$	0.33
2	$(NH_4)_6MO_7O_{24}.2H_2O$	0.88
3	KBr	1.2
4	KI	0.83
5	$ZnSO_4.7H_2O$	2.87
6	$Cd(NO_3).4H_2O$	1.55
7	$Co(NO_3)_2.6H_2O$	1.46
8	$CuSO_4.5H_2O$	1.25
9	$NiSO_4(NH_4)2SO_4.6H_2O$	1.98
10	$Cr(NO_3)_3.9H_2O$	0.41
11	V_2O_5	0.089
12	$AIK(SO_4)_2.12H_2O$	9.48
13	H_3BO_3	3.1
14	$MnSO_4.4H_2O$	2.23

Appendix II – Putative identifications of the MS/MS spectrums present in active samples

Table A.II 1 – Putative identification of unique mass peaks in active extracts in the Global Natural Products Social Molecular Networking (GNPS) platform, including direct identification from the molecular network, Dereplicator and Dereplicator +, Dictionary of Marine Natural Products (DMNP), and Dictionary of Natural Products (DNP). M, accurate mass; $M+H^+$, mass + hydrogen (parent mass); RT, retention time; ppm, parts per million.

Extract	$M+H^+$	RT	Putative identification / Compound class	m/z error (ppm)	Shared Peaks	MQScore	Formula	Source
2A	342.08	43.5334	Not identified					
2A	905.547	745.719	Not identified					
2A	731.495	762.561	Not identified					
2A	718.483	753.613	Not identified					
1B, 2A	715.464	746.610	Mytilus Inhibitory peptides; MIP-6 / Inhibitory hexapeptides	2.93			$C_{35}H_{58}N_{10}O_6$	DMNP
			Cholestane-3,6,15,24-tetrol; (3β,5α,6α,15α,24S)-form, 3-O-(2-O-Methyl-β-D-xylopyranoside), 24-O-α-L-arabinofuranoside / Steroidal glycosides	1.04			$C_{38}H_{66}O_{12}$	
1B	621.437	748.705	Bafilomycin A_1; 2-Demethoxy, 2-methyl, 19-Me / Macrolide antibiotics	0.56			$C_{36}H_{60}O_8$	DMNP
			Bafilomycin A_1; 2-Demethoxy, 2-methyl, 21-Me / Macrolide antibiotics					
			Bafilomycin A_1; 21-Deoxy, 19-Me / Macrolide antibiotics					
			12-Oleanene-3,16,28-triol; (3β,16β)-form, 3-*O*-β-D-Galactopyranoside / Pentacyclic triterpenoids					
			12-Oleanene-3,16,28-triol; (3β,16β)-form, 3-*O*-β-D-Glucopyranoside / Pentacyclic triterpenoids					
			Sipholenol C; 4-Ketone, 19 -*O*-α-L-rhamnopyranoside / Sipholane triterpenoids					

1B, 2A	528.193	35.471	Dapiramicin B / Nucleoside antibiotics	-2,26			$C_{21}H_{29}N_5O_{11}$	DNP
1B	510.3	609.273	Not identified					
1B, 2A	507.281	567.692	Cyclomarin A 13,14-Deepoxy, 13,14-didehydro, N50-de-Me / Cyclic heptapeptides					Dereplicator
2A	242.046	457.261	Tariacuripyrone / Natural nitro-compounds	2.74			$C_{13}H_7NO_4$	DNP
2A	763.467	1010.09	Not identified					
2A	749.451	932.272	Not identified					
1B	735.436	911.33	Not identified					
1B	555.284	709.494	Not identified					
1B	441.253	681.601	Not identified					
1B	397.226	687.038	Blastmycetin F / Teleocidin-related metabolites	5.12			$C_{22}H_{28}N_4O_3$	DNP
1B, 2A	294.183	732.873	Not identified					
2A	935.517	814.347	Not identified					
2A	935.517	816.034	Not identified					
1B	983.538	819.691	[D-Asp3,(E)-Dhb7] Microcystin LR / Cyclic heptapeptides					Dereplicator
1B	1830.07	822.021	Not identified					
2A	869.557	866.369	Not identified					
2A	868.545	852.368	Not identified					
1B, 2A	867.542	851.246	Virotoxin [Ala1] Viroidin / Cycloamanides					Dereplicator
1B	301.285	468.197	Not identified					
1B, 2A	1356.33	923.264	Not identified					
1B, 2A	1430.35	941.772	Petriellin A / Cyclic depsapeptides					Dereplicator
2A	773.534	1084.788	MassBank Record: LQB00261		6	0.766385		GNPS
2A	773.534	1086.07	Not identified					
2A	652.552	808.126	Not identified					
2A	623.509	728.39	Not identified					